

Aus der
Neurologischen Universitätsklinik Tübingen
Abteilung Neurologie mit Schwerpunkt Epileptologie

**Shear-Wave-Elastography in Neurofibromatosis Type I, II
and CIDP**

Inaugural-Dissertation
zur Erlangung des Doktorgrades der Medizin

der Medizinischen Fakultät
der Eberhard Karls Universität
zu Tübingen

vorgelegt von

Staber, Deborah Katharina

2024

Dekan: Professor Dr. B. Pichler

1. Berichterstatter: Privatdozent Dr. J. C. Marquetand
2. Berichterstatter: Privatdozent Dr. A. Lindner

Tag der Disputation: 10.09.2024

Table of Contents

1. Introduction	1
1.1. Shear-Wave-Elastography	1
1.1.1. Physical Background	1
1.1.2. Applications in daily clinical routine	5
1.1.3. Nerve Shear-Wave-Elastography	6
1.2. Diseases associated with peripheral nerve enlargement	10
1.2.1. Inflammatory nerve diseases – Model disease CIDP	13
1.2.2. Neoplastic enlargement – Model disease NF	16
1.3. Aims and hypotheses	21
2. Methods	21
2.1. Participants	22
2.1.1. B-mode imaging protocol	25
2.1.2. SWE measurement protocol	26
2.2. Statistic	29
3. Results	30
3.1. Sociodemographic Results	30
3.2. Normality distribution of all variables	31
3.3. Group Comparisons	32
3.4. B-mode Imaging	35
3.4.1. Neurofibroma in numbers	35
3.4.2. Nerve dimensions	37
3.5. SWE Results	42
3.5.1. Wrist position versus SWE	42
3.5.2. SWE of forearm and upper arm	47
3.5.3. SWV vs. number of neurofibroma in NF patients	53
4. Discussion	54
4.1. NF	55
4.2. CIDP	59
4.3. Ultrasound SWE	62
5. Summary	65
5.1. English Summary	66
5.2. German Summary - Deutsche Zusammenfassung	66
6. References	68
7. Declaration of own contribution	77
8. Own Publications	78
9. Acknowledgements	79

List of all figures:

1. Representation of longitudinal waves and transverse/shear waves in tissue.
2. Shear waves travelling through a stiff structure in body tissue.
3. Shear wave velocity imaging on an enlarged nerve.
4. SWV of tibial nerve with diabetic polyneuropathy.
5. Cystic radial nerve Schwannoma imaging.
6. Simplified comparison of a peripheral nerve in three states: healthy, CIDP and NF.
7. Cross-sectional B-mode ultrasound of median nerve in upper arm
8. Comparison of Control nerve and CIDP nerve of the median nerve in the upper arm in B-mode ultrasound.
9. Some NF1 diagnosis criteria.
10. Neurofibroma in conventional B-mode-ultrasound.
11. Representation of positioning of the transducer along the median nerve.
12. Wrist positioning and transducer positioning.
13. Forearm median nerve width in Control, NF and CIDP patients.
14. Forearm median nerve height in Control, NF and CIDP patients.
15. Upper arm median nerve width in Control, NF and CIDP patients.
16. Upper arm median nerve height in Control, NF and CIDP patients.
17. SWV of median nerve with wrist fully extended in Control, NF and CIDP group.
18. SWV of median nerve with wrist in neutral position in Control, NF and CIDP group.
19. SWV of median nerve with wrist fully flexed in Control, NF and CIDP group.
20. SWV of median nerve in the forearm.
21. SWV of median nerve in upper arm.
22. SWV (m/s) of median nerve in forearm and upper arm versus height (mm) and width (mm) of median nerve.
23. SWV (m/s) of median nerve in forearm with wrist in extension, neutral and flexion.

List of all tables:

1. A summary of the 2021 diagnostic criteria for typical CIDP and CIDP variants published by the European Academy of Neurology.
2. A summary of the characteristics gathered from the NF participants.
3. A summary of the characteristics gathered from the Control participants which were matched with the NF participants.
4. A summary of the characteristics gathered from the CIDP participants.
5. Summary of number of patients in all three patient groups; NF, Control and CIDP.
6. Sociodemographic results of BMI and age in all three patient groups; NF, Control and CIDP.
7. Shapiro-Wilk test results for all measurements taken across all three patient groups (NF, Control and CIDP).
8. Mann-Whitney U test results for all measurements taken across all three patient groups (NF, Control and CIDP).

9. Wilcoxon Test for all three wrist positions in all three patient groups (NF, Control and CIDP).
10. Number of neurofibroma counted in upper and lower arm as well as total number of neurofibroma on arm.
11. Comparison between participant groups in height (mm) and width (mm) of median nerve.
12. Height and width of median nerve in Control, NF and CIDP group.
13. SWV of median nerve in full extension wrist position in NF, Control and CIDP patient groups.
14. SWV comparison of median nerve across all 3 patient groups in extension wrist position.
15. SWV of median nerve in neutral wrist position in NF, Control and CIDP patient groups.
16. SWV comparison of median nerve across all 3 patient groups in neutral wrist position.
17. SWV of median nerve in full flexion wrist position in NF, Control and CIDP patient groups.
18. SWV comparison of median nerve across all 3 patient groups in flexion wrist position.
19. SWV of median nerve in forearm and upper arm in NF, Control and CIDP patient groups.
20. Comparison of the SWV (m/s) in the median nerve in the forearm and upper arm versus height and width of the nerve.
21. Comparison of the SWV (m/s) in the median nerve in extension, neutral and flexion wrist position vs total number of neurofibromas.
22. A summary of the external and internal factors which can influence ultrasound SWE calculations.

List of abbreviations:

USE =	Ultrasound elastography
NF =	Neurofibromatosis
NF1 =	Neurofibromatosis Type 1
NF2 =	Neurofibromatosis Type 2
CIDP =	Chronic inflammatory demyelinating polyneuropathy
SWE =	Shear wave elastography
SWV =	Shear wave velocity
BMI =	Body mass index
SD =	Standard deviation
Min. =	Minimum
Max. =	Maximum
FA =	Forearm
UA =	Upper arm
UPSS =	Ultrasound pattern sum score
CSA =	Cross sectional area
UPS-A =	Ultrasound pattern score A
UPS-B =	Ultrasound pattern score B
UPS-C =	Ultrasound pattern score C
Sig. =	Exact significance
U =	Mann Whitney U Test

vs. = Versus
PNT = Peripheral nerve tumour

1. Introduction

1.1. Shear-Wave-Elastography

1.1.1. Physical Background

Our nowadays well-known ultrasound imaging was first introduced into clinical settings in the 1970s (Campbell, 2013). Over the years the ultrasound modalities expanded and specialised in different directions, such as Doppler imaging, and further to ultrasound elastography in the 1990s (Gennisson et al., 2013). The latter can be considered as an objective tissue palpation performed by clinicians as it quantifies tissue elasticity, or simply said the stiffness of the body tissue. Amongst different types of elastography (Taljanovic et al., 2017), two forms are most used (Dietrich et al., 2017): (1) Compression elastography, also known as strain elastography, where tissue strain imaging is created by measuring tissue displacement under external pressure and (2) without external pressure, shear wave elastography (SWE) (Dietrich et al., 2017), where stiffness is calculated via measuring the speed of shear waves that transverse through tissue (Gennisson et al., 2013). This thesis will focus on SWE.

What are shear waves? When using ultrasound, sonic waves propagate longitudinally throughout the body tissue. SWE entails an additional use of waves that propagate at a 90° -angle to the longitudinal waves, i.e., transversally (Taljanovic et al., 2017). These transversal waves are also named shear-waves (Barr, Ferraioli, 2023) (see figure 1).

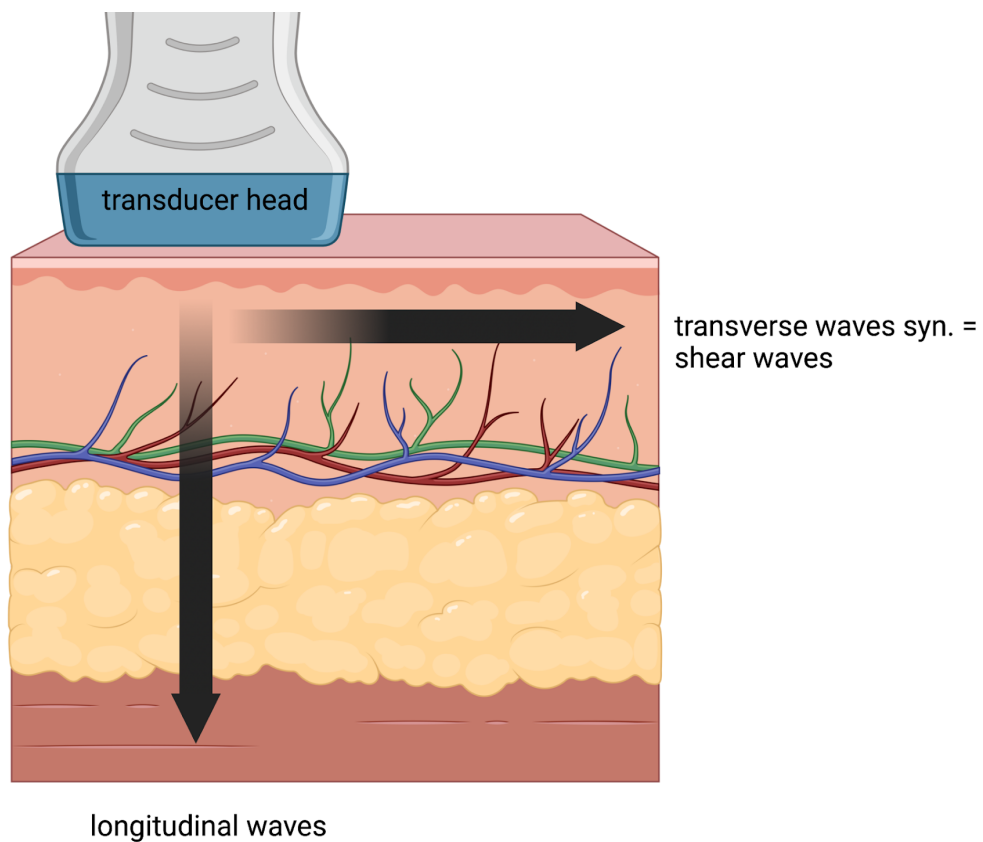


Figure 1. Representation of longitudinal waves and transverse/shear waves in tissue. (Own representation) The ultrasound transducer head sends longitudinal waves (left arrow) into the body tissue which results in the simultaneous emission of shear waves (right arrow) which travel through the body tissue perpendicularly from the longitudinal waves.

As the shear waves propagate through the tissue their speed will increase or decrease, depending on the elasticity of the tissue (see figure 2).

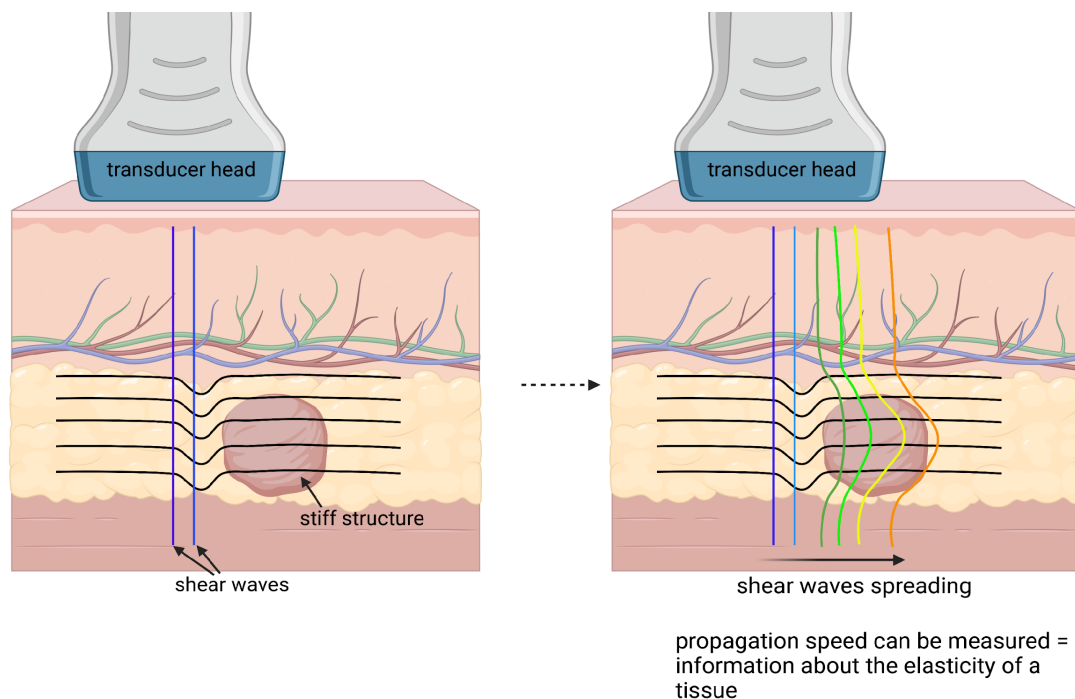


Figure 2. Shear waves travelling through a stiff structure in body tissue. (Own representation) The ultrasound transducer head emits the shear waves which transverse through the body tissue. (In this representation the shear waves are travelling from left to right). Once the shear waves reach the stiff structure the shear waves alter their propagation speed which can be measured and then used to calculate the elasticity of the stiff structure.

The velocity of the shear waves travelling through the tissue is measured and then depicted as colours in the imaging (Gennisson et al., 2013), i.e., a rainbow colour spectrum from blue to red (see figure 3). Where there is softer tissue, the shear waves travel at a slower speed, which are conventionally closer to the colour blue on the spectrum. Where the tissue is stiffer, the shear waves can travel faster and are closer to the colour red on the spectrum (Akagi and Kusama, 2015) (Bouillard et al., 2011) (see figure 3).

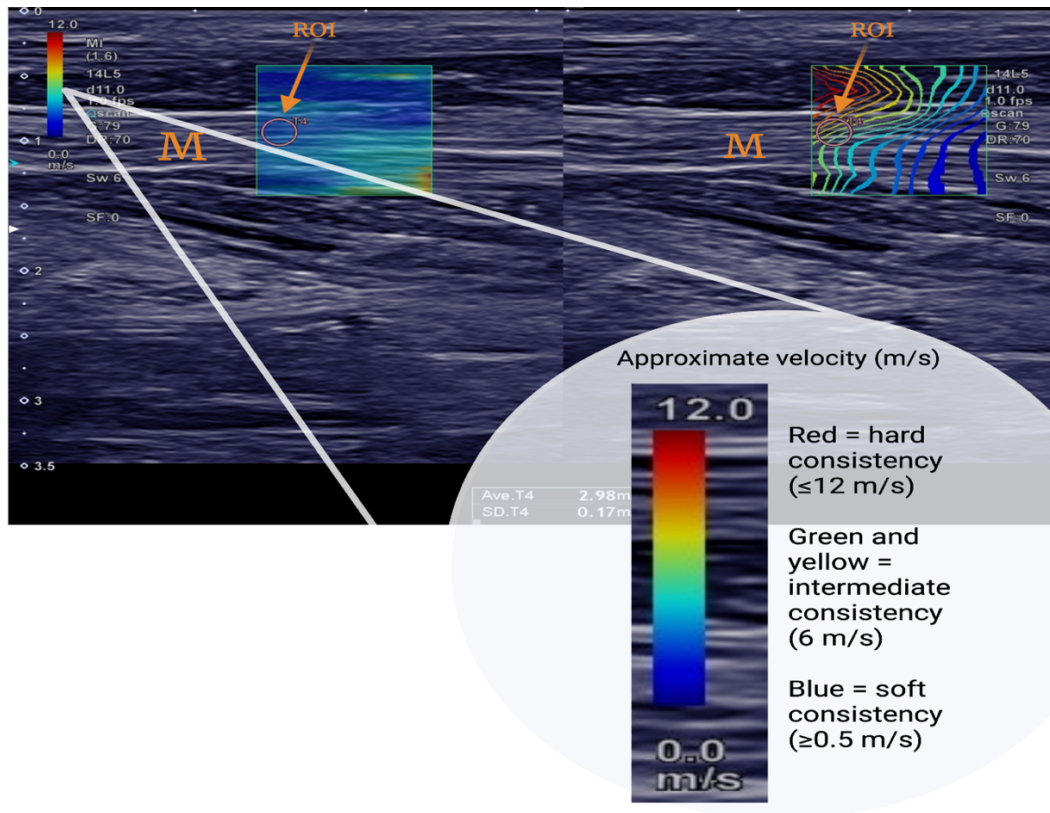


Figure 3. Shear wave velocity imaging on an enlarged nerve. (Own representation) The median nerve will be the nerve studied throughout all cases in this study. In this figure, the nerve is enlarged due to chronic inflammation demyelinating polyradiculoneuropathy (CIDP). The B-mode imaging in grey is overlaid with SWV colour data (the square coloured box). The closer to blue on the colour spectrum, the slower the shear wave speed measured. 'M' labels the median nerve. The ROI (Region of interest) is displayed as an orange circle. The colours represent the approximate velocity measured of the shear waves in the median nerve. The red colour indicates a hard consistency, with an approximate speed of 12 m/s, green and yellow indicate an intermediate consistency of approximately 6 m/s while blue indicates a softer consistency with a shear wave velocity of approximately ≥ 0.5 m/s.

When the shear wave velocity (SWV) has been measured, the tissue elasticity can then also be calculated, (when assumed a linear elastic behaviour) by using the following equation for shear elastic modulus (μ) in kPa, where $\mu = \rho V_s^2$ (Bouillard et al., 2011): ρ = tissue density (kg/m^3), V_s = SWV (m/s). Using this

equation, it is shown that when the stiffness increases (in this case; the shear elastic modulus) the SWV also increases (Leong et al., 2019).

1.1.2. Applications in daily clinical routine

In daily clinical routine, ultrasound elastography (USE) is used across the spectrum assessing the elasticity of homogenous organs, such as the liver (Barr et al., 2015), thyroid (Hu et al., 2017) or breast (Gong et al., 2011). Here, the increased elasticity or stiffness due to fibrosis or tumours can be assessed.

As an example, categorising stages of liver fibrosis using SWE is possible and poses a non-invasive alternative to biopsy and histopathological evaluation, which is currently the standard procedure to evaluate liver fibrosis staging. Liver biopsies are invasive and come with complications such as a haemorrhage (0.3%) or even death (0.01%) (Zaki et al., 2019) while, SWE, being non-invasive, can image the approximate estimate of the liver tissue elasticity in real time. Next to the assessment of fibrosis, SWE is also used as an additional method to characterize tumour dignity of breast, liver, thyroid and prostate tumours (Gennisson et al., 2013) (Barr et al., 2015) (Ferraioli et al., 2018) (Cosgrove et al., 2012). Cancer cells have a different structure and composition to healthy cells, such as increased collagen and others proteins that contribute to the stiffness of malignant tissue, which makes malignant tissue usually stiffer (Nižetić and Groet, 2012). The circumstance that tumour tissue is stiffer than the surrounding tissue has been used as an advantage for centuries using manual palpation, e.g., feeling the breast tumour when palpating the breast. Here, SWE offers an objective method (unlike palpation) and visualisation of the malignant tissue. Also, for the application of SWE in characterising tumours, SWE provides data which enables clinicians to obtain values regarding the stiffness of tissue in real time (without an invasive procedure) or over a period with repeated measurements to monitor tumour growth. Especially in breast tumours, SWE has come so far as to have a scoring system based on SWE results. For example, the Tsukuba score is a system used to evaluate the likelihood that a breast lesion is malignant based on SWE. It considers four different characteristics of the

lesion: shape, margin, echo pattern, and posterior acoustic features. Each characteristic is assigned a score from 1 to 5, with 1 indicating a low likelihood and 5 indicating a high likelihood of cancer. The scores for each characteristic are then added up to give a total score between 4 and 20. A higher score indicates a greater likelihood of cancer, while a lower score indicates a lower likelihood. Lesions with a total score of 4 or 5 are considered low-risk and may not require biopsy, while those with a score of 16 or higher are considered high-risk and are more likely to require biopsy or further testing (Itoh et al., 2006) (Barr, 2015). Here the Tsukuba score showed 88.3% accuracy (Itoh et al., 2006) (Barr et al., 2015). The Tsukuba score sensitivity and specificity when differentiating the malignant from the benign lesions were both high at 86.5% and 89.9% (Itoh et al., 2006). Not only did SWE perform well as a non-invasive method of categorizing lesions in breast tissue, SWE had a better diagnostic performance than B-mode-ultrasound and Doppler imaging for the characterisation of thyroid nodules (Hazem et al., 2021.) and even showed significant difference between prostate cancer and benign prostate tissue with a statistically significant correlation with the Gleason score ($r=0.898$, $p<0.0001$) (Shoji et al., 2018) (Ageeli et al., 2021) (Woo et al., 2014). The Gleason score grades prostate cancer cells based on their microscopic appearance and ranges from 1-5 based on two prominent patterns in a biopsy. Higher scores indicate more aggressive cancers that may require more aggressive treatment (Epstein et al., 2005). The Gleason score being used with SWE shows that not only can SWE be used to make scores which could help with diagnostic and staging, like the Tsukuba score, but can also be used alongside already existing scores and diagnostic methods.

1.1.3. Nerve Shear-Wave-Elastography

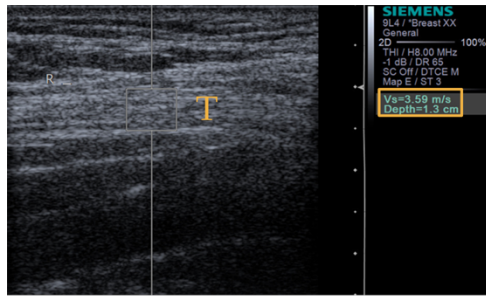
Shear wave elastography (SWE) has been investigated in studies on nerve compression syndromes and diabetic neuropathy even though it has not been established in daily clinical routine. Carpal tunnel syndrome (CTS) has been the focus of several studies on nerve compression syndromes [25] [26] [27] [28]. Diagnosis of CTS is mainly based on clinical information such as symptoms and

signs, as well as physical examinations, with the nerve conduction study being the gold standard. Also, conventional B-mode ultrasound imaging can be used for diagnosing CTS, which typically shows a nerve thickening, which is due to nerve swelling and connective tissue changes, which may be caused by chronic compression or inflammation of the nerve. As the nerve shows changes in thickness, this could affect the elasticity which in turn could potentially be estimated using SWE. Studies found median nerve stiffness, cross-sectional area, and vascularity of the median nerve were significantly different between CTS and Control wrists ($p < 0.04$) [28]. In addition, the mild-to-moderate and severe CTS groups had increased median nerve stiffness in the wrist and forearm compared to Controls ($p < 0.001$) [27], and the nerve cross-sectional area and stiffness increased in relation to the electrodiagnostic testing severity of CTS [26]. This means the more severe the CTS the stiffer and thicker the nerve. A study published by Nam et al. (Nam et al., 2021) demonstrated that SWE provided accurate measurements of median nerve stiffness and the authors concluded that SWE might be a valuable diagnostic tool for CTS, with 96% accuracy and 100% specificity. Similarly, Wee and Simon used SWE to differentiate the severity of CTS ($p = .008$) while suggesting SWE could be implemented as an additional diagnostic tool (Wee and Simon, 2020). Next to CTS, studies have also investigated the use of SWE for diagnosing cubital tunnel syndrome (Nam et al., 2021). Kim and Lee conducted a study using SWE to evaluate the ulnar nerve and discovered that it was effective in diagnosing ulnar neuropathy due to cubital tunnel syndrome. SWE provided quantitative measurements of nerve stiffness and could identify the affected nerve segment, making it a valuable diagnostic tool (Nam et al., 2021). Furthermore, SWE could not only identify the affected nerve segment, but also differentiate between cubital tunnel syndrome and medial epicondylitis. SWE distinguished between these two conditions with a specificity of 100% and a sensitivity of 80% (Wee and Simon, 2020).

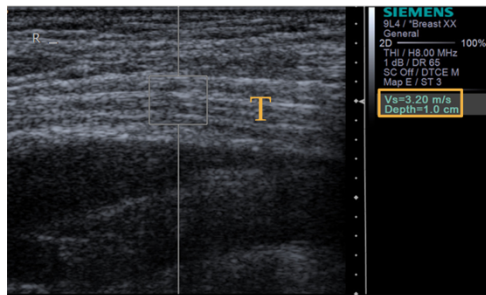
The mentioned studies on CTS and cubital tunnel syndrome highlight the use of ultrasound imaging in detecting and evaluating nerve compression syndromes, as it has been shown to identify significant differences in nerve thickness and

stiffness. Potentially, SWE could be integrated in daily clinical settings, particularly in cases where nerve conduction studies may be inconclusive or not readily available.

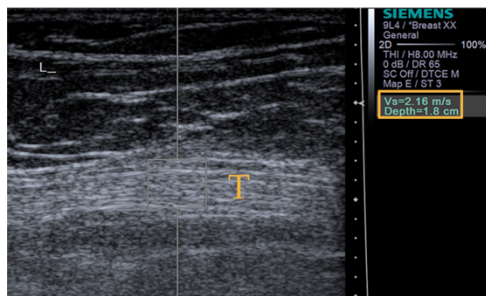
Alongside nerve compression syndromes, diabetic neuropathy has also been investigated where SWE was used in the evaluation of peripheral neuropathies in diabetic patients. Patients with diabetic peripheral neuropathy have high blood sugar levels which may cause axonal swelling resulting in thickened nerves (Riazi et al., 2012) (Liu et al., 2012) (Cartwright et al., 2008). This could affect the stiffness for the nerves which could be estimated using SWE. Wie et al. assessed the tibial nerve stiffness using SWE in patients with diabetic peripheral neuropathy. For a visual representation of the tibial nerves refer to figure 4. Tibial nerve stiffness values within the patient group (with and without diabetic peripheral neuropathy) were all significantly higher than in the Control group ($p < .05$) but not significantly thicker ($p > .05$) (Wei and Ye, 2020). The authors concluded that SWE could be a method for detecting peripheral neuropathy in diabetic patients (sensitivity 63.33% and specificity 92.5%) and proposed nerve SWE for monitoring disease progression (Wei and Ye, 2020).



Tibial nerve using SWE of 50-year-old female **control** participant.
SWV: 3.59 m/s



Tibial nerve using SWE of 53-year-old male patient with newly diagnosed **diabetes without diabetes polyneuropathy**.
SWV: 3.20 m/s



Tibial nerve using SWE of 65-year-old patient **diabetes** for 20 years and **diabetes polyneuropathy**.
SWV: 2.16 m/s

Figure 4. SWV of tibial nerve with diabetic polyneuropathy. (modified from Wei et al. (Wei and Ye, 2020)) SWV of the tibial nerve in Control, patients with diabetes but without diabetes polyneuropathy and patients with diabetes as well as diabetes polyneuropathy. The orange “T” marks the tibial nerve in the ultrasound image. The orange square shows the calculated SWV.

Furthermore, SWE has been utilised in the diagnostic of nerve tumours. SWE was used to evaluate a cystic radial nerve Schwannoma. The authors found that SWE distinguished the cystic lesion from the surrounding normal nerve tissue (76% sensitivity and 64% specificity) in diagnosing malignancy (Battaglia et al., 2017) indicating its potential as a diagnostic tool for nerve tumours however did not describe whether the SWE was higher, lower or similar when malignant (see figure 5). Even with such encouraging results when evaluating peripheral nerves, it is important to note that it is not yet a standard procedure in daily clinical routine.

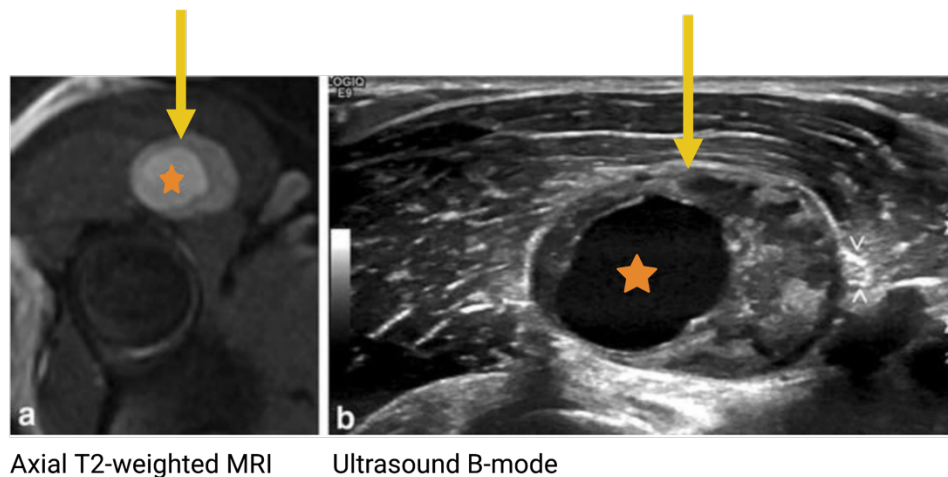


Figure 5. Cystic radial nerve Schwannoma imaging. (modified from Battaglia et al. (Battaglia et al., 2017)) Visual representation of radial nerve Schwannoma (yellow arrows. The prominent internal cyst (orange star) that is hyperintense with T2-weighting and hypoechoic ultrasound. No SWE maps were provided in the study.

1.2. Diseases associated with peripheral nerve enlargement

Peripheral nerve enlargement can be a symptom of a wide range of diseases and conditions, including infective, non-infective (e.g., autoimmune or paraproteinemic), tumours such as peripheral nerve tumours (PNTs), hereditary, or even trauma. For example, leprosy is an infectious condition caused by *Mycobacterium leprae* in which the enlarged peripheral nerve is central to the diagnosis (Merlini et al., 2011) (Staber et al., 2022). In this case, the nerve, such as the ulnar nerve, is palpable and visible due to a superficial perineural osteo fibrotic reaction of the nerve tissue (Khadilkar et al., 2015). Hereditary peripheral nerve enlargement, such as localized hypertrophic neuropathy, can also result in an increase in CSA of nerves, including the femoral and proximal ulnar nerve (Staber et al., 2022).

Enlarged peripheral nerves can be examined and diagnosed using different modalities, such as the ultrasound pattern sum score (UPSS), which can be used when identifying and differentiating between acute and chronic neuropathies. The UPSS is the sum of three cross-sectional sub-scores (A, B and C): UPS-A (sensorimotor nerves), UPS-B (cervical and vagal nerve) and UPS-C (sural

nerve) (Grimm et al., 2015). UPSS can be used to differentiate between acute inflammatory demyelinating polyneuropathy (AIDP or Guillain–Barré syndrome) and chronic inflammatory demyelinating polyneuropathy (CIDP). (The latter will be discussed in section 1.2.1. and 4. 2.) Additionally, other modalities such as MRI are used to detect nerve enlargement and complement ultrasound imaging, particularly in enlarged proximal or deeper nerve segments that may not be studied using ultrasound adequately (Donaghy, 2003) (Winter et al., 2017). This is because the image sharpness, and therefore quality, decreases as depth increases due to attenuation, scattering, and diffraction. The ultrasound waves lose intensity, get deflected in different directions, and bend as they pass through small openings. The trade-off of more depth comes with lower quality of imaging (Battaglia et al., 2017).

Another reason why a nerve may be thicker can be due to PNTs (see figure 6 and 7). Here the increase in thickness can occur when there is a physical displacement of nerve fibres and changes in the microenvironment surrounding the affected nerve (Kim et al., 2009). While B-mode-ultrasound has advantages in detecting PNTs, differentiating between schwannoma, neurofibroma, and malignant degeneration can be challenging without biopsy and histology due to limitations in the imaging including identifying tissue and cell types. However, there have been studies aimed at addressing this limitation in B-mode-ultrasound (Eichelmann et al., 2013; Winter et al., 2017). Nevertheless, PET and MRI imaging are recommended to differentiate precisely between malignant and benign PNTs.

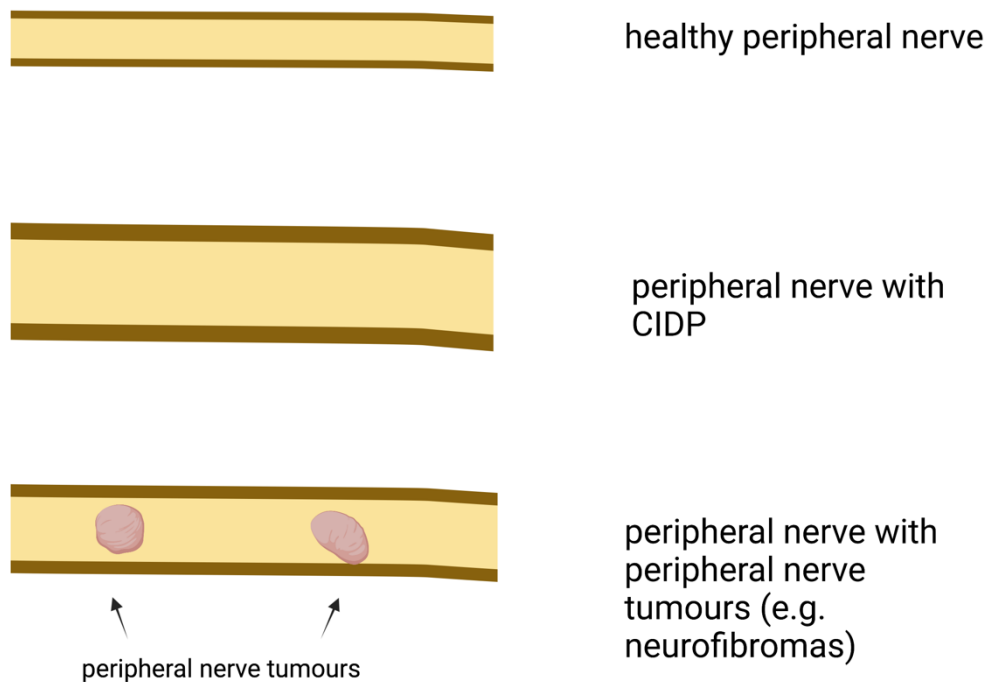


Figure 6. Simplified comparison of a peripheral nerve in three states: healthy, CIDP and NF. (Own representation) The healthy nerve shows no abnormalities. The CIDP nerve is much thicker to demonstrate the inflammatory nerve disease CIDP, an enlarged nerve without PNTs. The NF nerve, also thicker than that of the Control nerve, shows two PNTs which in this case are neurofibromas, an enlarged nerve due to PNTs.

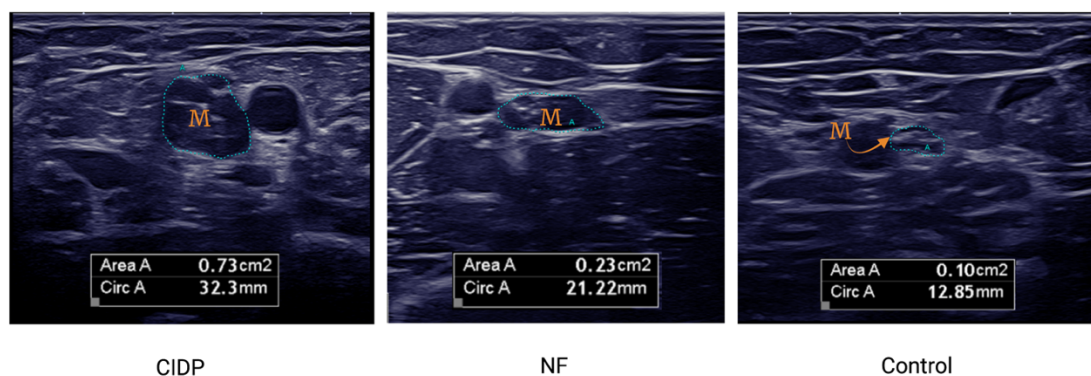


Figure 7. Cross-sectional B-mode ultrasound of median nerve in upper arm. (Own representation) Here the cross-sectional areas of the median nerve in the upper arm are compared between CIDP, Neurofibromatosis (NF) and a Control. The blue dotted line shows the outline of the median nerve, and the orange 'M' is to show where the median nerve is. Each picture has a box in the middle bottom with 'Area A' which means cross sectional area and 'Circ A' which means circumference. Notice that the CIDP (0.73cm²) and the NF (0.23cm²) nerve have a higher cross-sectional area than that of the Control (0.10cm²).

1.2.1. Inflammatory nerve diseases – Model disease CIDP

The term 'inflammatory nerve diseases' is broad and to understand this spectrum, diseases can be utilised as a model disease to represent the spectrum. A model disease is a well-studied disease that is used in research to understand its underlying mechanisms, develop therapeutic interventions, and helps advance our understanding of biological systems. In this case, CIDP, the most common chronic immune-mediated inflammatory polyneuropathy (Lehmann et al., 2019), will be the model disease for inflammatory nerve diseases causing nerve thickness (see figure 6 and 7).

CIDP is a peripheral nerve disorder characterised by enlarged and thicker nerves due to inflammation and demyelination of the affected nerves (Lehmann et al., 2019). The immune system reacts to the myelin sheath surrounding the peripheral nerves, resulting in nerve enlargement and thickening. As 90% of patients with CIDP have thicker nerves (Di Pasquale et al., 2015) it could be possible to examine the nerves using SWE but currently studies are lacking. Conventionally the inflamed nerves can be visualised using B-mode ultrasound. A typical example of a median nerve with CIDP is seen below for reference with a healthy median nerve for comparison (see figure 8).

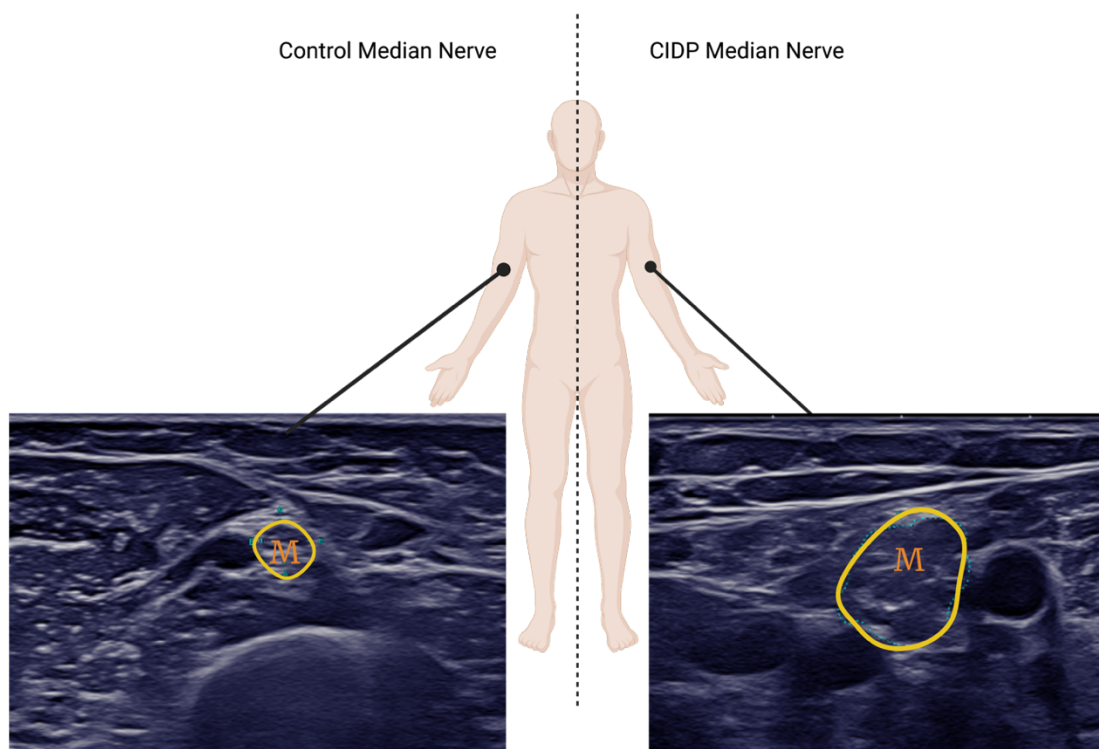


Figure 8. Comparison of Control nerve and CIDP nerve of the median nerve in the upper arm in B-mode ultrasound. (Own representation) Here it can be seen that the median nerve (M) in the upper arm of the CIDP nerve is thicker than that of the Control median nerve. The median nerve in both cases has been given a yellow border for easy identification. Note: although this figure shows measurements from both left and right arm, both measurements were taken from the right arm in both Control median nerve and CIDP median nerve.

Furthermore, using ultrasound, like seen in figure 8, a diagnostic criterion can be used to diagnose CIDP and determine which kind of CIDP is present. In 2021, the European Academy of Neurology suggested to use ultrasound imaging to diagnose adults with CIDP (there is currently no evidence for paediatric patients). If there is a nerve enlargement in two or more sites in proximal median nerve segments and/or the brachial plexus, then a CIDP diagnosis is more likely. The European Academy of Neurology state that nerve enlargement is defined by cross-sectional area median nerve of $>10 \text{ mm}^2$ at forearm, $>13 \text{ mm}^2$ upper arm, $>9 \text{ mm}^2$ interscalene (trunks) or $>12 \text{ mm}^2$ for nerve roots. The above mentioned ultrasound criteria compliment the electrophysiological criteria for CIDP, which essentially require signs of demyelination in multiple nerves (Van den Bergh et al., 2021). In addition, a diagnostic criterion for CIDP was also published by the

European Academy of Neurology which allowed for the CIDP diagnosis to be broken down into typical CIDP and CIDP variants (Van den Bergh et al., 2021) (see table 1).

Typical CIDP All the following:	CIDP Variants Minimum of one of the following:
Progressive or relapsing, symmetrical, muscle weakness of all limbs, and sensory involvement of at least two limbs	Distal CIDP: distal sensory loss and muscle weakness predominantly in lower limbs
Increasing symptoms over at least 8 weeks	Multifocal CIDP: sensory loss and muscle weakness in a multifocal pattern, usually asymmetric, upper limb predominantly and usually first to show symptoms, in more than one limb.
Absent or reduced deep tendon reflexes in all joints.	Focal CIDP: sensory loss and muscle weakness in only one limb, most common in the brachial or lumbosacral plexus
	Motor CIDP: motor symptoms and signs without sensory involvement
	Sensory CIDP: sensory symptoms and signs without motor involvement

Table 1. A summary of the 2021 diagnostic criteria for typical CIDP and CIDP variants published by the European Academy of Neurology. (Own representation)

Clinical symptoms of typical CIDP and the above mentioned CIDP variants include (see table 1), but are not limited to, progressive and symmetrical muscle

weakness in both the proximal and distal proximities, loss of reflexes, compromised balance as well as loss of sensory function (Dimachkie and Barohn, 2013). The prevalence lies at around 0.33 per 100,00 adults and most are first aware of their symptoms between 30 to 60 years of age (Broers et al., 2019). CIDP can occur in a stepwise progression or as spontaneous remissions (Hirst et al., 2006). A diagnosis is normally made upon an extensive anamnesis, nerve examinations such as biopsies, nerve conduction studies and sometimes even cerebrospinal fluid analysis (Drulović et al. 1996). Between 69% to 100% of patients with CIDP prove to have nerves with a larger diameter (Zaidman and Pestronk, 2014a).

The European Academy of Neurology recommends a principal treatment for both subtypes of CIDP with intravenous immunoglobulin or corticosteroids (Van den Bergh et al., 2021). These can be used for maintenance treatment too. Should this not have an effect then a plasma exchange should be undergone. Should a maintenance dosage become too high then combination treatments or the addition of immunosuppressants or immunomodulatory drugs should be highly considered. Intravenous Immunoglobulin works particularly well as therapy for patients with motor CIDP (Van den Bergh et al., 2021) (see table 1). Should no treatment be undergone, or the CIDP is not recognised, patients risk becoming wheelchair bound, therefore CIDP should be diagnosed correctly and furthermore, treated correctly too (Spina et al., 2017).

1.2.2. Neoplastic enlargement – Model disease NF

While CIDP is the model disease for inflammatory disease enlargement without PNTs, Neurofibromatosis (NF) is the model disease for neoplastic enlargement. To be precise, NF distinguished into two main subtypes: NF type 1 (also known as Recklinghausen's disease) (Ghalayani et al., 2012) and NF type 2.

1.2.2.1. *Neurofibromatosis Type 1*

Amongst the two main subtypes, NF1 is the more common of the two subtypes, as NF1 occurs in 1:3000 while NF2 is present in 1:25,000 people (Korf, 2013). NF1 is autosomal dominant, shows a complete penetrance amongst the patients (Korf, 2013) and has a 100% penetrance, meaning that every person with this gene mutation shows NF1 symptoms.

Regarding symptoms, NF1 tend to present as, but not limit itself to, symptoms such as Café-au-lait macules, optic gliomas, skinfold freckles, peripheral nerve sheath tumours and as previously mentioned alongside cognitive impairment (HOU et al., 2020) (see figure 9). For an NF1 diagnosis, two or more of the following criteria must be fulfilled; more than six Café-au-lait macules, two or more lisch nodules (well defined, brown elevations on the iris surface of the eye (Lubs et al. 1991), plexiform neurofibromas of the nodules, optic gliomas, an osseous lesion, axillary or inguinal freckling (Boyd et al., 2009) and a first degree relative with NF1 (Senthilkumar and Tripathy, 2023).

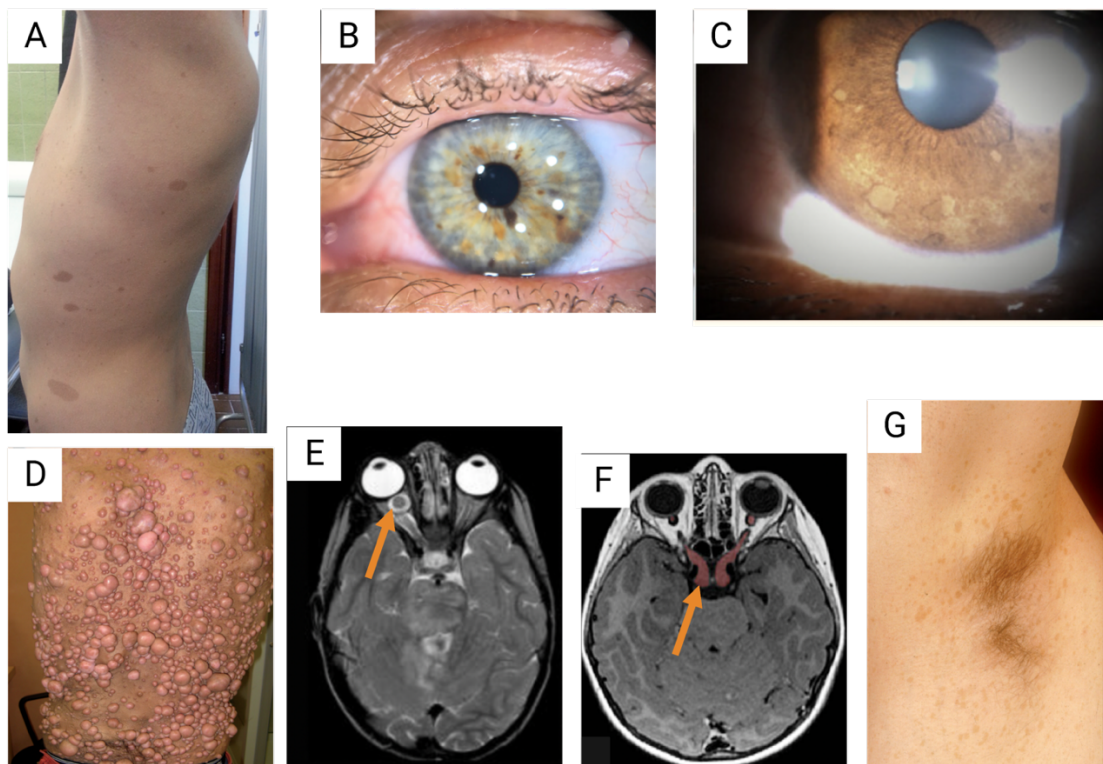


Figure 9. Some NF1 diagnosis criteria. (modified from Miraglia et al. (Miraglia et al., 2020), Bouirig et al. (Bouirig and Cherkaoui, 2022), Antonioli et al. (Antonioli et al., 2021), Campen et al. (Campen and Gutmann, 2018) and Blank et al. (Blank et al., 2017)) A: Café-au-lait macules.,

B: lisch nodules, C: lisch nodules, D: plexiform neurofibromas of the nodules, E: optic gliomas (orange arrow indicating the optic glioma on the optic nerve), F: optic gliomas gliomas (orange arrow indicating the optic glioma on the optic nerve and optic chiasma.) Here the optic glioma is marked as red, G: axillary freckling.

Symptoms range widely and while some patients feel local pain due the enlarged nerve compressing the nerve or other anatomical structures within the body. Some patients have many yet unnoticeably (for the patient) small neurofibromas while other patients exhibit only a few, in comparison, very large neurofibromas which are easily palpated.

The two main causes of deaths amongst NF1 patients are glioma and malignant deformation of neurofibroma (Evans et al., 2011), however NF has no preference to sex or nationality (Ghalayani et al., 2012) (Evans et al., 2011). In epidemiological studies, cardiovascular disease has been reported to be four times more likely in NF1 males, while in NF1 females showed breast cancer to be five times more likely due to the downregulations of the oncogene ras due to a mutation of the NF1 gene (Suarez-Kelly et al., 2019) (Evans et al., 2011). 52% women had enlarged neurofibromas, while 64% had growth of new neurofibromas during their pregnancy, as well as more complications (Murray and Shapiro, 2010). It is argued that the increase in oestrogen and progesterone influence the growth and malignant transformation of the neurofibromas (Well et al., 2020).

The pathophysiology of NF1 is complex. NF1 stems from a gene mutation situated on chromosome 17 which codes for a Ras-GTPase activating protein named neurofibromin-1 (Korf, 2013). This protein's function is to regulate cell proliferation and differentiation so in turn acts as a tumour suppressor (Simanshu et al., 2017). A malfunctioning protein can allow the cell to grow uncontrollably resulting in tumours, so called neurofibromas. Neurofibromas have fibroblasts, mast cells, schwann cells, perineuronal cells and axons within their extracellular matrix. In addition, neurofibromin-1 also attaches to microtubules important for the release of adenylyl cyclase, which is important for cognition (HOU et al.,

2020). This role in cognition may explain why NF1 patients may show learning disabilities or difficulties at school at a young age (“Learning disabilities in children with neurofibromatosis type 1: subtypes, cognitive profile, and attention-deficit-hyperactivity disorder - PubMed,” n.d.). Up to 60% of children with NF1 show form of learning difficulties during school years. Most tumours remain benign however can cause discomfort and damage to surrounding tissues due to the compression (Ouiminga et al., 2019).

Additionally, in conventional B-mode-ultrasound, neurofibromas are classically described as having a hypoechoic structure (see figure 10), with a detectable central hyper-echogenicity ("target sign") (Reynolds et al., 2004). This phenomenon is not always seen in B-mode ultrasound.

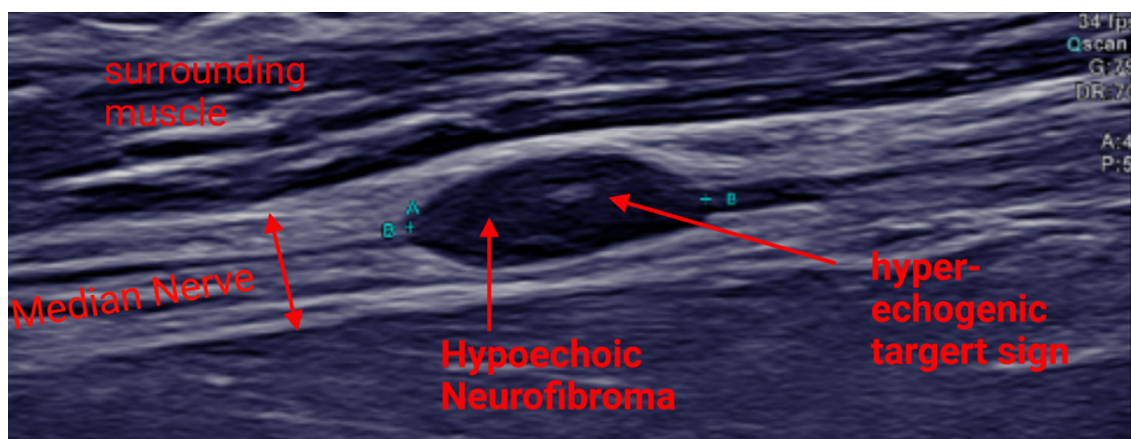


Figure 10. Neurofibroma in conventional B-mode-ultrasound (Own representation) Depicted is the median nerve with a hyperechoic neurofibroma which also shows a hyperechogenic target sign.

1.2.2.2. Neurofibromatosis Type 2

NF2, as known as ‘central NF’, as it tends to manifest especially along the central nervous system (Miettinen et al., 2017). NF2, less common than NF1, can occur when a mutation of the merlin gene arises and is autosomal dominant. NF2 patients have a higher rate of new mutations while half of NF1 patients bear a new mutation.

Within the NF2 diagnosis there are a further 2 two main subtypes, although they will not be distinguished between in this thesis, they shall be briefly explained. The Wishart type is the more aggressively progressive type with on onset of symptoms before the age of 20 and the Gardner type has a later symptom beginning and lower tumour count (Ruggieri et al., 2016). NF2 patients either have a bilateral schwannoma or have a one-sided schwannoma before the age of 30 with a member of the first-grade family with NF2. In addition, patients can be diagnosed NF2 when one has 2 or more of the following: meningioma, astrocytoma, glioblastoma, ependymoma, schwannoma, juvenile posterior subcapsular lens opacification, glial haematuria (Evans, 2009).

Like NF1, NF2 pathophysiology is also complex. The NF2 gene is located on Chromosome 22, which inactivates the cytoskeletal merlin protein, a tumour suppressor, which is vital for a cell's signalling pathways and, like neurofibromin, controls the cell's division and growth (Surace et al., 2004). Without this protein, the schwannomas can grow uncontrollably. Typical characteristics for NF2 patients are the bilateral vestibular schwannomas resulting in hearing loss due to their invasive nature (Stangerup et al., 2006) (Korf, 2013). It is not known why NF2 associated vestibular schwannomas are common since current research (Stangerup et al., 2006) regarding schwannoma growth from sporadic vestibular schwannoma cannot be applied to NF2 because of a higher proliferation index (Antinheimo et al., 1995) (Saito et al., 2003) and less vascularisation. Like NF1, the tumours are commonly noncancerous yet do however require a degree of monitoring through examination, symptoms, and medical imaging to ensure no malignancy is overlooked.

At present , there is no cure for NF patients (Korf, 2013). However, if some tumours become too large, and therefore cause the patient discomfort or in fact grow to become malignant, the tumours can be removed via surgery. If the tumours become malignant radiation and chemotherapy can also be offered. For patients with hearing loss due to NF, cochlear implants as well as auditory brainstem implants are possible. Again, like CIDP and NF1, early diagnosis and

precise monitoring with effective therapy are essential for patient comfort and outcome.

1.3. Aims and hypotheses

The aim of this thesis is to investigate the extent to which enlarged peripheral nerves show altered elasticity and determine whether SWE used for this purpose can distinguish between two model peripheral nerve diseases; nerve enlargement because of nerve tumours (NF) and nerve enlargement because of inflammation (CIDP).

The following hypotheses were challenged:

(1) There is a significant difference between NF1, NF2 and CIDP regarding nerve SWE. As thickness of the nerve positively correlates with the SWV it is expected that CIDP has the highest SWV, followed by NF and the healthy Control nerves with the lowest SWV.

(2) Nerve enlargement, be it because of tumours (NF) or inflammation (CIDP), alter the shear wave velocity (SWV) during different biomechanically evoked positions of the median nerve using three conditions of the wrist joint: zero-degree, maximal flexion, and maximal extension.

It is expected that more extended the nerve, the higher the SWV, the more flexed the nerve, the lower the SWV.

(3) Neurofibromas found in NF1 and NF2 have a different SWE than that of a healthy nerve. It is expected that the SWV will be higher in the neurofibromas than that of the healthy nerve.

2. Methods

2.1. Participants

Although Covid-19-pandemic was present, access to the hospital as well as research facilities were restricted, and participants and patients were frightened of exposing themselves to COVID-19, 15 healthy Controls, 15 patients with NF and 7 CIDP patients were found willing to participate in the study. Amongst the NF patients, 11 patients had NF 1 and 4 had NF 2. All participants were 18 years old or older and had signed an informed consent document. This study has the approval from the ethics committee (77072020BO2, 18/11/2020) of the University of Tübingen and the examinations aligned with the Declaration of Helsinki.

NF patients were selected at the neurology department in the University Hospital of Tübingen. Patients with NF in the median nerve from a previous study (Winter et al., 2017) were contacted and asked to participate. Amongst both NF 1 and NF 2, there was an average age of 32.9 years and average BMI was 24.54 kg/m² (see table 2).

Participant	Age (years)	Height (cm)	Weight (kg)	BMI (= kg/m²)	Sex (F/M)	Diagnosis (NF1=1, NF2=2)
NF1	22	160	62	24.2	F	1
NF2	33	159	70	27.7	F	1
NF3	32	150	70	31.1	F	2
NF4	66	179	82	25.6	M	2
NF5	21	153	55	23.5	F	1
NF6	21	168	57	20.2	F	1
NF7	48	162	70	26.7	M	1

NF8	24	166	60	21.8	F	2
NF9	32	160	48	18.8	F	1
NF10	27	176	61	19.7	M	1
NF11	24	178	78	24.6	M	1
NF12	30	168	64	22.7	F	1
NF13	51	185	90	26.3	M	1
NF14	42	163	63	23.7	F	2
NF15	21	187	110	31.5	M	1

Table 2. A summary of the characteristics gathered from the NF participants. F = Female. M = Male.

Next, a Control participant was found for each NF patient matched by sex and gender for a direct comparison. The average age was 35.2 years old and average BMI was 26.15 kg/m² with nine females and six males (see table 3).

Participant	Age (years)	Height (cm)	Weight (kg)	BMI (= kg/m ²)	Sex (F/M)
K1	23	168	62	22	F
K2	34	170	104	36	F
K3	70	176	128	41.3	M
K4	66	175	75	24.5	M
K5	21	178	68	21.5	W
K6	20	163	54	20.3	W

K7	53	183	90	26.9	M
K8	24	172	68	23	W
K9	27	169	62	21.7	W
K10	27	183	83	24.8	M
K11	23	189	75	21	M
K12	34	173	75	21	W
K13	45	183	85	25.4	M
K14	42	178	135	42.6	W
K15	20	176	63	20.3	W

Table 3. A summary of the characteristics gathered from the Control participants which were matched with the NF participants.

Like the NF patients, the CIDP patients were recruited at the neurology department in the University Hospital of Tübingen. The CIDP patients were contacted if they had a known UPSS of over 6. This group had an average age of 71.6 years old and an average BMI of 27.14 kg/m² with 2 females and 5 males (see table 4).

Participant	Age (years)	Height (cm)	Weight (kg)	BMI (= kg/m²)	Sex (F/M)
CIDP1	82	175	87	21	M
CIDP2	78	180	84	25.9	M
CIDP3	61	180	80	24.7	F

CIDP4	51	172	63	21.3	F
CIDP5	69	183	115	34.3	M
CIDP6	73	184	104	30.7	M
CIDP7	87	172	95	32.1	M

Table 4. A summary of the characteristics gathered from CIDP participants.

Both CIDP and NF patients, as well as healthy Controls, were seated on the same chair, with the right arm supported on a cushion for a standardised position with the back of the hand on the cushion and elbow flexed around 120° flexion in the elbow. By making the participants sign a waiver it was ensured that all healthy Controls had no other/additional neuromuscular disease.

2.1.1. B-mode imaging protocol

The right median nerve was measured using conventional B-Mode-ultrasound (Canon Aplio i800 device with a 14 MHz linear transducer, i14LX5/PLI-1205BX, Canon Medical Systems, Neuss, Germany).

Firstly, all participants, (NF, CIDP and Control) had the right median nerve examined from the from the flexor retinaculum to the axilla. Next, the nerve height and width were measured 3cm proximal from the flexor retinaculum. Patients with NF had nerve height and width measured where there were no visible neurofibromas.

Furthermore, the NF patients had the neurofibromas along their right median nerve counted using B-mode ultrasound. The neurofibromas were counted from the proximal end of the flexor retinaculum of the hand up to the start of the axilla. The largest neurofibroma in the lower arm (B in figure 11) and upper arm (C in figure 11) were chosen for further SWE measurements. The two largest

neurofibromas had height, width and length measured, with volume also being calculated.

2.1.2. SWE measurement protocol

After locating the neurofibromas with B-mode as mentioned above, SWE was used to measure the median nerve as well as the elasticity of the neurofibromas. To ensure the examined arm was as relaxed as possible, participants were asked to not undertake any vigorous exercise before the appointment. This prevented activated muscles compressing the median nerve resulting in possibly slightly different measurements.

The SWE settings were as following: size of the region of interest (ROI): 2, ROI shape: radius, frame rate: 1, time smoothing: 0 (no time averaging), map type: speed (display of the shear wave velocity in meters per second).

On the display screen, a square over the B-mode image of the nerve appears to indicate where the measurement is being taken. The aim was to find the most homogenous area of nerve, which in propagation mode was visualised by coloured bands. The start of the tracking was coloured blue and the end with an orange to red colour. In addition, a colour-coded map was shown indicating the general homogeneity of the selected nerve tissue. The aim was to obtain a homogenous blue colour in the colour-coded map, and this was then used to select a uniform area of nerve tissue to measure. Here, the nerve fibres ran parallel to one another. A homogeneous area of nerve tissue is important to make sure the standard deviation was not too high, and measurements obtained were more accurate. To prevent probe-induced stiffness, attention was paid when applying the minimal sufficient pressure to the probe and to increase surface area as well as contrast enhancement ultrasound gel was used (Kim et al., 2008).

Firstly, the SWV of a neurofibroma free section of the median nerve, 3cm proximal of the flexor reticulum (A in figure 11) was measured. Subsequently, the

SWV of the two largest neurofibromas were measured lengthwise (strictly one in the lower (B in figure 11) and the other in the upper arm (C in figure 11)).

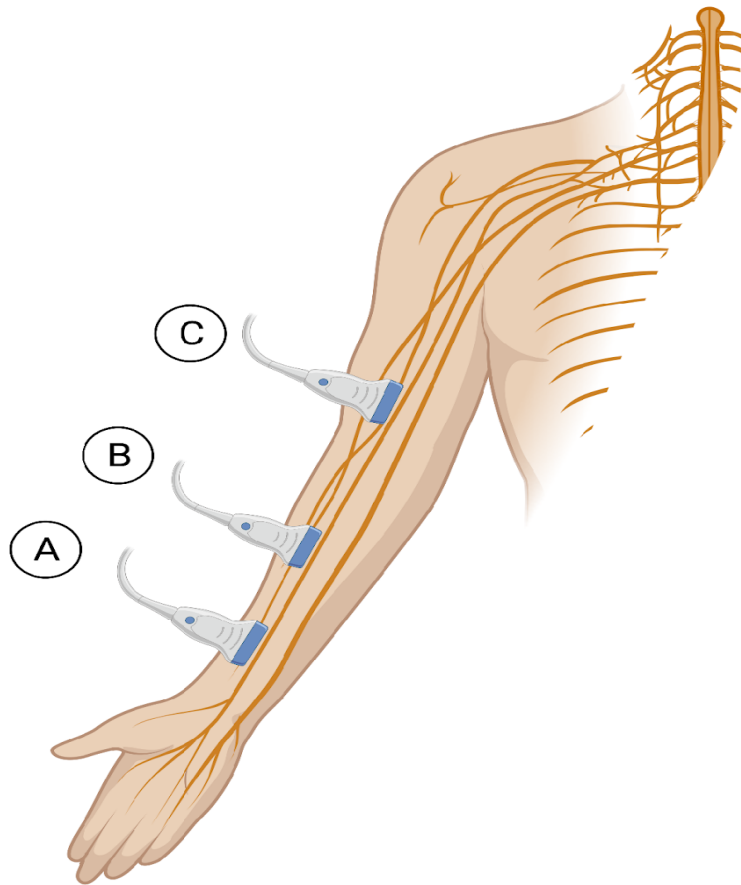


Figure 11. Representation of positioning of the transducer along the median nerve. (Own representation) Three positions were used to measure the SWE of the median nerve. Position A was positioned 3cm proximal from the flexor retinaculum in three wrist positions: zero-degree, individual maximal flexion, and extension. Position B was a measurement taken in the largest neurofibroma in the lower arm (below elbow) and C, the largest neurofibroma in the upper arm (above elbow).

To assess the extent neurofibroma alters the shear wave velocity (SWV) of the median nerve, all participants were asked to perform the following three conditions in the wrist joint: zero-degree, individual maximal flexion, and extension (see figure 12). Measurements were also carried out in a neurofibroma-free area of the median nerve and with the transducer positioned strictly 3cm

proximal from the flexor retinaculum (A in diagram above). This was to investigate whether the pathological nerve (pathological nerve segment without neurofibroma) of the NF patient was different from that of their healthy Control.


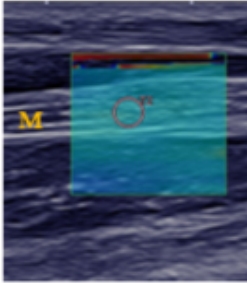
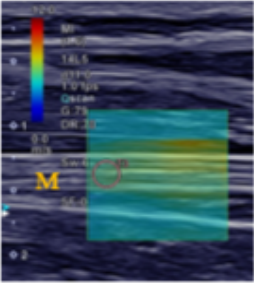

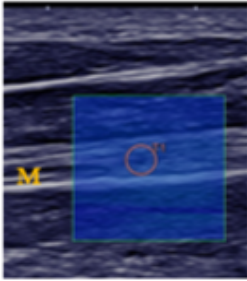
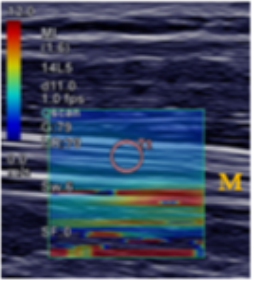

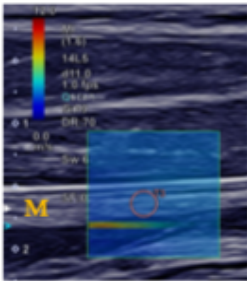
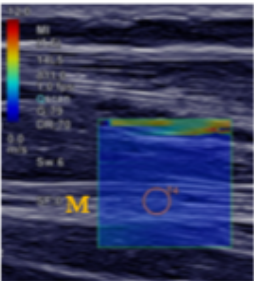
	Position	SWV in an NF patient	SWV in a healthy control
Extension			
Neutral null position			
Flexion			

Figure 12. Wrist positioning and transducer positioning. (modified from Staber et al. (Staber et al., 2022)) SWE of the median nerve in extension, neutral position, and flexion of the wrist in patients with neurofibromatosis and healthy Controls. The orange “M” marks the median nerve in the ultrasound image. The orange circle marks the field of measurement.

The Control participants had the same measurements taken as the NF patients. SWE of their median nerve was measured (strictly once in the lower and the other in the upper arm) to mirror the two measurements of the two largest neurofibromas measured in the NF patients.

It should be noted that three NF patients had difficulty hearing. For these patients, the instructing of wrist movements and general communication was performed in written form with pen and paper.

2.2. Statistic

The statistical analysis of the collected data was performed with the Statistical Package for the Social Sciences (SPSS) version 28 for MacOS, IBM Corporation, Armonk, NY, USA.

For nerve related measurements (such as height, length, volume of neurofibromas) and sociodemographic results descriptive statistics were computed – including the mean, median, range, minimum, maximum, standard deviation, and variance.

Normal distribution was tested using Shapiro-Wilk test for the variables upper arm width, SWV median nerve extension, SWV median nerve neutral, SWV median nerve flexion, forearm SWV median nerve lengthwise, forearm median nerve height, forearm median nerve width, upper arm SWV median nerve lengthwise and upper arm median nerve height in CIDP, NF and Control participants. Due to the smaller sample sizes, most of the data was not normally distributed.

Therefore, Mann Whitney U Tests were used to test for significant differences in SWE between patient groups (NF vs Control, NF vs CIDP, CIDP vs NF) for SWV median nerve extension, SWV median nerve neutral, SWV median nerve flexion, forearm median nerve height, forearm median nerve width, forearm SWV

lengthwise, upper arm SWV lengthwise, upper arm median nerve height and upper arm median nerve width.

Additionally, differentiation in the variance in NF, Control and CIDP participants for wrist position (neutral vs extension, extension vs flexion, neutral vs flexion) were tested for using the Wilcoxon Signed Rank test. For all tests, the significance level was set to $p < 0.05$ and all graphs were created using SPSS.

Finally, Spearman's rho correlation was used for all three patient groups in forearm and upper arm for BMI vs. SWV lengthwise as well as for CIDP UPSSS vs. SWE.

3. Results

3.1. Sociodemographic Results

The total of 37 patients throughout all three patient groups were divided into three patient groups: 15 NF patients (NF1 = 11, NF2 = 4), 15 matched Control patients and 7 CIDP patients (see table 5).

Group	Number of Patients
NF1	11
NF2	4
NF Total	15
Control	15
CIDP	7
Total	37

Table 5. Summary of number of patients in all three patient groups; NF, Control and CIDP.

Amongst all three patient groups, the CIDP patients had the highest mean BMI of 27.14 kg/m² and the highest mean age of 68.43 years. The mean BMI of the NF and the matched Control group was 24.54 kg/m² and 26.15 kg/m², while the

mean age of the NF and Control was 33.27 years and 35.87 years (see table 6). Average age of onset in NF1 and NF2 symptoms are much lower than that of CIDP at around 20 years of age (Evans, 1998) (Ferner et al., 2007).

	Group	Mean	SD	Variance	Median	Min.	Max.	Range
BMI	NF	24.54	3.76	14.17	24.20	18.8	31.5	12.7
	Control	26.15	7.53	56.63	23	20.3	42.6	22.3
	CIDP	27.14	5.29	27.97	25.90	21	34.3	13.3
Age	NF	33.27	14.31	204.64	30	20	66	46
	Control	35.87	16.24	263.70	33	20	69	49
	CIDP	68.43	10.88	118.29	69	50	82	32

Table 6. Sociodemographic results of BMI and age in all three patient groups; NF, Control and CIDP. BMI = body mass index kg/m². SD= standard deviation. Min. = Minimum. Max.= Maximum.

3.2. Normality distribution of all variables

Normal distribution was tested using the Shapiro–Wilk test (see table 5).

	Group	Shapiro-Wilk Sig.	Normal distribution?
Upper arm width (mm)	Control	0.023	No
	NF	0.029	No
	CIDP	0.009	No
SWV median nerve extension (m/s)	Control	0.320	Yes
	NF	0.123	Yes
	CIDP	0.519	Yes
SWV median nerve neutral (m/s)	Control	0.058	Yes
	NF	0.599	Yes
	CIDP	0.430	Yes

SWV median nerve flexion (m/s)	Control	0.149	Yes
	NF	.258	Yes
	CIDP	<0.001	No
Forearm SWV median nerve lengthwise (m/s)	Control	0.010	No
	NF	0.005	No
	CIDP	0.074	No
Forearm median nerve height (mm)	Control	0.374	Yes
	NF	0.126	Yes
	CIDP	0.166	Yes
Forearm median nerve width (mm)	Control	0.019	No
	NF	0.007	No
	CIDP	0.452	Yes
Upper arm SWV median nerve lengthwise (m/s)	Control	0.104	Yes
	NF	0.185	Yes
	CIDP	0.452	Yes
Upper arm median nerve height (mm)	Control	0.526	Yes
	NF	0.009	No
	CIDP	0.779	Yes

Table 7. Shapiro-Wilk test results for all measurements taken across all three patient groups (NF, Control and CIDP).

Generally, normality could not be assumed due to the small sample sizes. The Shapiro–Wilk test was significant for several measurements including the height of the median nerve in the upper arm in Control patients ($p = 0.526$) and CIDP patients ($p = 0.779$) and the SWV of the median nerve lengthwise in the upper arm in Control, NF and CIDP patients ($p = 0.104$, $p = 0.185$, $p = 0.452$). For all tests, the significance level was set to $p < 0.05$.

3.3. Group Comparisons

It was also tested whether there was a difference in SWV of the median nerve between the NF, CIDP and healthy Control groups, as unpaired samples, using the Mann–Whitney U test with a significance level of $p < 0.05$. Everything below 0.05 was considered as a significant difference. SWE was tested for each of the different positions (flexion, extension, and neutral) (see table 8).

	Control vs. NF		NF vs. CIDP		CIDP vs. Control	
	Mann-Whitney (U)	Sig. (p)	Mann-Whitney (U)	Sig. (p)	Mann-Whitney (U)	Sig. (p)
SWV median nerve extension (m/s)	56.500	0.190	72.000	0.185	50.000	0.891
SWV median nerve neutral (m/s)	44.500	0.004	69.000	0.267	42.000	0.490
SWV median nerve flexion (m/s)	84.500	0.250	53.500	0.945	45.000	0.630
Forearm median nerve height (mm)	106.000	0.806	64.000	0.447	86.000	0.017
Forearm median nerve width (mm)	81.500	0.202	88.000	0.011	99.000	0.000

Forearm SWV lengthwise (m/s)	55.000	0.160	31.000	0.142	52.000	1.000
Upper arm SWV lengthwise (m/s)	90.000	0.367	44.000	0.581	50.000	0.891
Upper arm median nerve height (mm)	132.500	0.412	71.000	0.021	98.000	0.001
Upper arm median nerve width (mm)	118.000	0.838	62.000	0.535	85.500	0.017

Table 8. Mann-Whitney U test results for all measurements taken across all three patient groups (NF, Control and CIDP). All p values which are significant are in bold. 'vs.' means versus. Sig. = Significance.

For Control vs. NF only the SWV (m/s) of median nerve in neutral position was significantly higher ($p = 0.004$) in the Control than the NF. For CIDP vs. Control the forearm median nerve height (mm) was significantly higher ($p = 0.017$) in CIDP, forearm median nerve width (mm) was significantly higher ($p = 0.000$) in CIDP, upper arm median nerve height (mm) was also significantly higher ($p = 0.001$) in CIDP, and upper arm median nerve width (mm) was significantly wider ($p = 0.017$) in CIDP.

For the Wilcoxon test, the significance level was set to $p < 0.05$. For the first test, comparing Neutral vs. Extension, all three groups showed a significant difference with p-values of 0.005 for NF, <0.001 Control, and 0.018 for CIDP (see table 9). This shows that the SWE in extension is significantly higher than in neutral. For the second test, comparing Extension vs. Flexion, all three groups also showed

a significant difference with p-values of 0.002 for NF, <0.001 for Control, and 0.018 for CIDP. This shows that the SWE was significantly higher in extension than it was in flexion. For the third test, comparing Neutral vs. Flexion, only the Control group showed a significant difference with a p-value of 0.011. The other two groups, NF and CIDP, did not show a significant difference with p-values of 0.125 and 0.128, respectively. This means that only in the Control group, the SWE was significantly higher in neutral than in flexion.

Patient group	SWE Neutral vs. Extension		SWE Extension vs. Flexion		SWE Neutral vs. Flexion	
	Wilcoxon Test (Z)	Sig. (p)	Wilcoxon Test (Z)	Sig. (p)	Wilcoxon Test (Z)	Sig. (p)
NF	-2.840	0.005	-3.067	0.002	-1.533	0.125
Control	-3.294	<0.001	-3.408	<0.001	-2.528	0.011
CIDP	-2.366	0.018	-2.366	0.018	-1.521	0.128

Table 9. Wilcoxon Test for the SWE in all three wrist positions in all three patient groups (NF, Control and CIDP).

3.4. B-mode Imaging

3.4.1. Neurofibroma in numbers

The number of neurofibroma in the forearm and the upper arm of NF patients were counted using B-mode ultrasound. Two patients, NF7 and NF10, had so many neurofibromas on both forearm and upper arm that it proved impossible to count how many neurofibromas were exactly present. Therefore, once 100 neurofibromas had been counted, the counting was then stopped and stated as over 100 (>100) neurofibromas in the forearm and over 100 (>100) in the upper arm (see table 10). These two patients are described as 'statistical outliers'.

Participant	Number of neurofibroma in forearm	Number of neurofibroma in upper arm	Number of Neurofibroma total
NF1	18	12	30
NF2	9	10	19
NF3	5	3	8
NF4	6	5	11
NF5	11	8	19
NF6	5	6	11
NF7	>100	>100	>200
NF8	8	8	16
NF9	6	9	15
NF10	>100	>100	>200
NF11	40	35	75
NF12	15	7	22
NF13	5	9	14
NF14	5	7	12
NF15	29	25	54

Table 10. Number of neurofibroma counted in upper and lower arm as well as total number of neurofibroma on arm.

3.4.2. Nerve dimensions

For the Control and CIDP group the median nerve was measured for height and width. However, in the NF group the neurofibroma was measured in height and width as well as length.

Parameter	NF vs. Control	Control vs. CIDP	CIDP vs. NF
Height (mm) of median nerve in forearm	U = 106 <i>p</i> = 0.806	U = 86 <i>p</i> = 0.017	U = 64 <i>p</i> = 0.447
Height (mm) of median nerve in upper arm	U = 132.5 <i>p</i> = 0.412	U = 98 <i>p</i> = 0.001	U = 71 <i>p</i> = 0.021
Width (mm) of median nerve in forearm	U = 81.5 <i>p</i> = 0.202	U = 99 <i>p</i> = 0.000	U = 88 <i>p</i> = 0.011
Width (mm) of median nerve in upper arm	U = 118 <i>p</i> = 0.838	U = 85.5 <i>p</i> = 0.017	U = 62 <i>p</i> = 0.535

Table 11. Comparison between participant groups in height (mm) and width (mm) of median nerve. The comparisons in bold are significant. U = Mann Whitney U test. *p* = Significance.

In table 11, when comparing NF and Control participants there were no significant differences between the height and width in the forearm or upper arm. When comparing the Control and CIDP groups, the CIDP group had significantly thicker median nerves in the forearm (height *p* = 0.017, width *p* = 0.000) as well as in the upper arm (height *p* = 0.001, width *p* = 0.017). When comparing the CIDP and the NF groups, the median nerve had a significantly larger height in the upper arm for the NF group (*p* = 0.021) and a significantly higher width (*p* = 0.011) of the median nerve in the forearm for the CIDP group.

Participant Group	Median nerve	Dimension	Mean	SD	Variance	Median	Min.	Max.	Range
Control	FA	Width (mm)	4.58	0.80	0.63	4.40	3.7	6.8	3.1
NF			4.28	2.79	7.76	3	1.4	12.2	10.8
CIDP			6.66	1.22	1.50	6.4	5.3	8.5	3.2
Control		Height (mm)	3.13	0.40	0.16	3.1	2.5	3.7	1.2
NF			3.26	1.89	3.58	2.6	1	7.4	6.4
CIDP			3.91	0.66	0.44	4.2	3	4.6	1.6
Control	UA	Width (mm)	4.67	1.60	2.57	4.6	0.09	6.7	6.61
NF			6.25	3.86	14.92	5	2	14.60	12.6
CIDP			6.21	2.06	4.25	6.6	1.8	7.7	5.9
Control		Height (mm)	3.47	0.59	0.35	3.4	2.6	4.8	2.2
NF			5.13	3.61	13.04	3.8	1	12.9	11.9
CIDP			4.82	0.63	0.40	4.8	3.91	5.6	1.69

Table 12. Height and width of median nerve in Control, NF and CIDP group. All measurements in mm. Min. = minimum. Max. = maximum. FA = forearm. UA = upper arm.

The CIDP group had a larger mean median nerve width (6.66 mm) in the forearm than the NF (4.28 mm) and Control group (4.59 mm). The Control group had the

smallest range in width of median nerve (3.1 mm), closely followed by CIDP (3.1 mm) and NF (10.8 mm) (see table 12 and figure 13).

Like in the forearm, the CIDP group had the highest mean height of the median nerve (3.91 mm), followed by the NF group (3.26 mm) and the Control group (3.133 mm) (see table 12 and figure 14). However, the NF group showed the highest range of height due to the neurofibromas (6.4mm).

In the forearm the CIDP patients had a greater mean nerve width. The neurofibromas vary more in height than width and the Control group have the lowest variance in terms of height and width in the forearm.

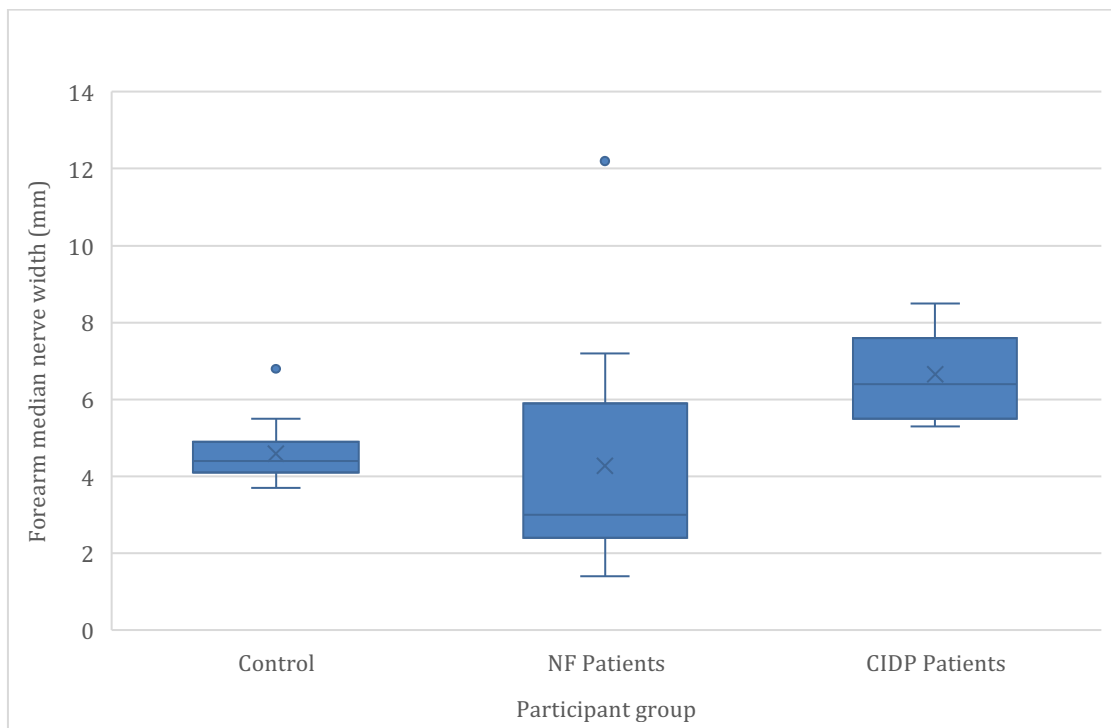


Figure 13. Forearm median nerve width in Control, NF and CIDP patients. (Own representation)

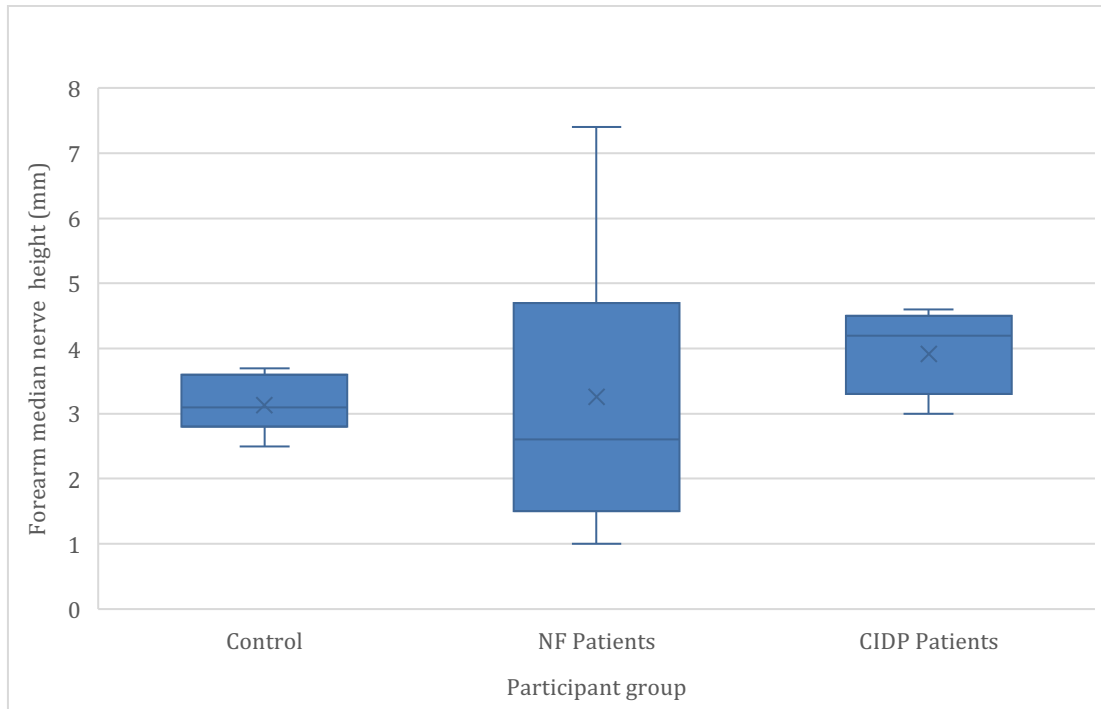


Figure 14. Forearm median nerve height in Control, NF and CIDP patients. (Own representation)

In the upper arm, NF patients had the highest mean width of the median nerve at 6.25 mm with Control at 4.67 mm and CIDP at 6.21 mm. Again, like in the forearm, the NF group show the greatest range in width due to the PNTs. The CIDP group had a smaller range (5.9 mm) that that of the Control group (6.61 mm) and the NF group (12.6 mm) (see table 12 and figure 15).

Regarding the height of the median nerve in the upper arm, the NF group had the largest range (11.9 mm), the NF group had the largest height measurement (5.13 mm), followed by CIDP (4.82 mm) and Control (3.47 mm). Here, the range was also smaller (1.69 mm) than that of the NF (11.9 mm) and Control group (2.2 mm) (see table 12 and figure 16).

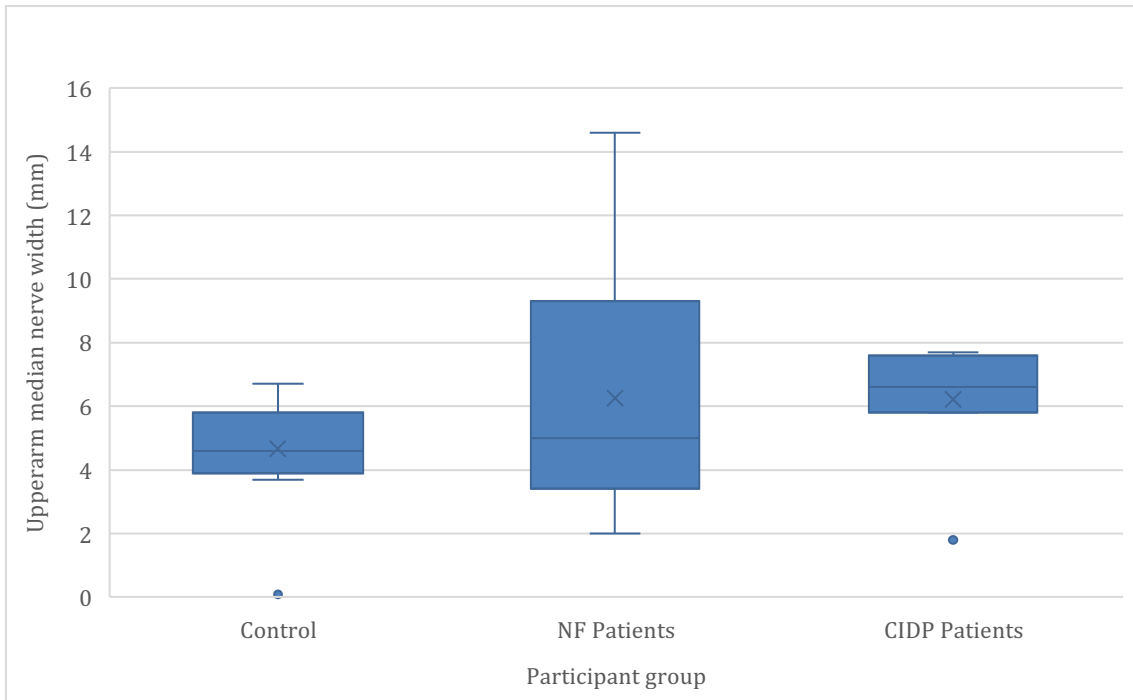


Figure 15. Upper arm median nerve width in Control, NF and CIDP patients. (Own representation)

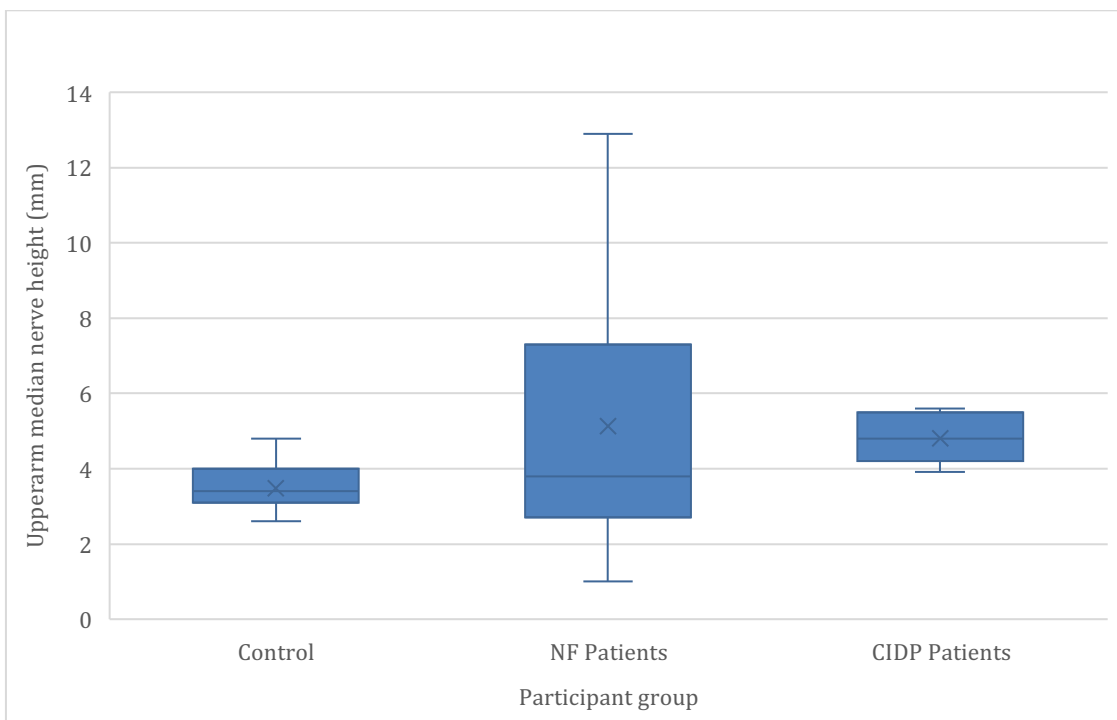


Figure 16. Upper arm median nerve height in Control, NF and CIDP patients. (Own representation)

3.5. SWE Results

3.5.1. Wrist position versus SWE

To investigate whether the wrist position influenced the SWE, the SWV was measured in the median nerve, with the wrist from all CIDP, NF and Control participants placed in three positions: full extension, neutral and full flexion.

3.5.1.1. SWE in extension

The SWE in extension was carried out in all three patient groups: Control, NF and CIDP.

Participant Group	Mean SWV (m/s)	SD	Variance	Median	Min.	Max.	Range
Control	5.63	1.30	1.67	5.53	3.45	7.79	4.34
NF	4.45	1.27	1.62	4.54	2.02	7.41	5.39
CIDP	5.78	1.82	3.32	5.69	3.86	8.62	4.76

Table 13. SWV of median nerve in full extension wrist position in NF, Control and CIDP patient groups. All measurements are in m/s. SD = standard deviation. Min. = minimum. Max. = maximum.

Wrist position	SWV (m/s) comparison of median nerve				
	NF (with outliers) vs. CIDP	NF (without outliers) vs. CIDP	CIDP vs. Control	NF (with outliers) vs. Control	NF (without outliers) vs. Control
Extension	U = 72 $p = 0.185$	U = 63 $p = 0.183$	U = 55 $p = 0.891$	U = 56.5 $p = 0.019$	U = 42.5 $p = 0.01$

Table 14. SWV comparison of median nerve across all 3 patient groups in extension wrist position. 'vs' means versus, 'U' means Mann Whitney U Test., 'p' means exact significance. Two NF outlier participants had over 100 neurofibromas. Significance was calculated with and without the outliers in comparisons. Significance values in bold are significant.

Table 13 and 14 suggest that in the extension wrist position, there are no significant differences in SWV between NF (with or without outliers) and CIDP. However, there are significant differences in SWV between both NF groups and the Control group with ($p = 0.019$) and without outliers ($p = 0.01$).

In full extension of the wrist position, the median nerve showed similar mean results in the Control (5.63 m/s) and the CIDP group (5.78 m/s), while the CIDP patient the greatest variance (3.32 m/s), while NF had the smallest variance (1.62 m/s) and Control (1.67 m/s). The NF group had the smallest variance as mentioned above, the smallest mean SWV (4.45 m/s) yet the largest range due to three statistical outliers (see table 13 and figure 17).

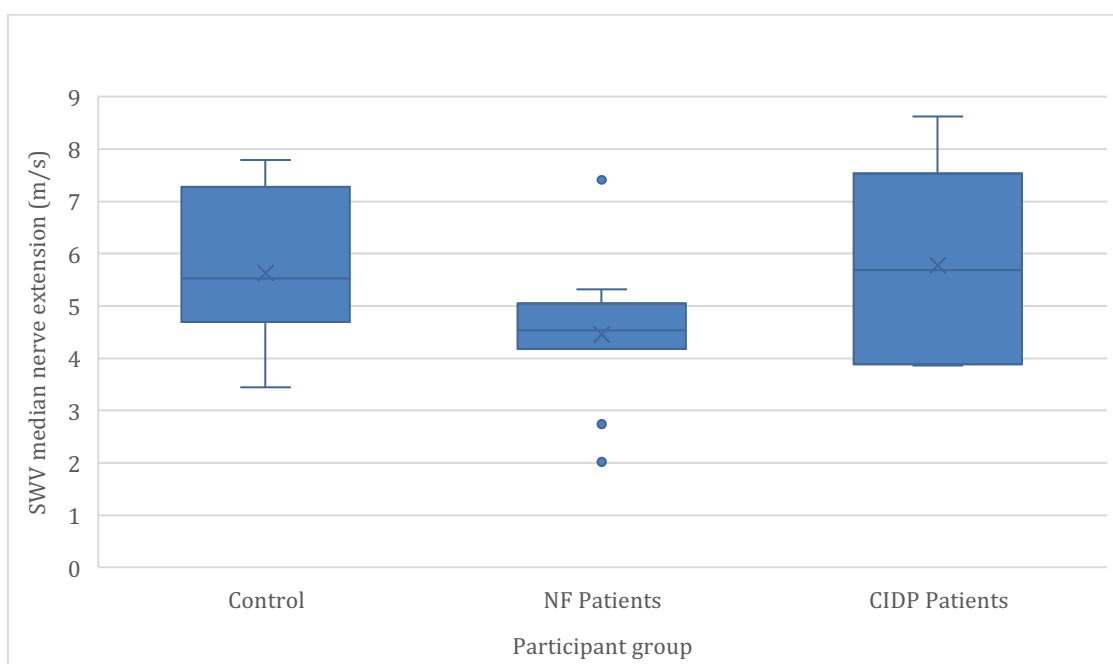


Figure 17. SWV of median nerve with wrist fully extended in Control, NF and CIDP group. (Own representation) SWV is in m/s.

3.5.1.2. SWE in neutral

The SWE in neutral was also carried out in all three patient groups: Control, NF and CIDP.

Participant Group	Mean SWV (m/s)	SD	Variance	Median	Min.	Max.	Range
Control	3.81	1.06	1.12	3.53	2.44	6.43	3.99
NF	2.83	0.66	0.44	2.72	1.86	4.03	2.17
CIDP	3.64	1.56	2.44	3.25	1.93	6.57	4.64

Table 15. SWV of median nerve in neutral wrist position in NF, Control and CIDP patient groups. All measurements are in m/s. SD = standard deviation. Min. = minimum. Max. = maximum.

Wrist position	SWV (m/s) comparison of median nerve				
	NF (with outliers) vs. CIDP	NF (without outliers) vs. CIDP	CIDP vs. Control	NF (with outliers) vs. Control	NF (without outliers) vs. Control
Neutral	U = 69 $p = 0.267$	U = 62 $p = 0.211$	U = 42 $p = 0.490$	U = 44.5 $p = \mathbf{0.004}$	U = 35.5 $p = \mathbf{0.002}$

Table 16. SWV comparison of median nerve across all 3 patient groups in neutral wrist position. 'vs' means versus, 'U' means Mann Whitney U Test., 'p' means exact significance. Two NF outlier participants had over 100 neurofibromas. Significance was calculated with and without the outliers in comparisons. Significance in bold are significant.

The results from tables 15 and 16 show that in a neutral wrist position, there are no significant differences in SWV between NF and CIDP (with or without outliers) or between CIDP and the Control group (with or without outliers). However, there are significant disparities in SWV when comparing NF, with ($p = 0.004$) and without outliers ($p = 0.002$), with the Control group.

In the neutral wrist position, the Control group had the highest mean SWV (3.81 m/s) when compared to NF (2.83 m/s) and CIDP (3.64 m/s). The NF group showed the smallest variance (0.44 m/s) compared to Control (1.12 m/s) and NF (0.44 m/s). CIDP had a lower minimum (1.93 m/s) (see table 15 and figure 18).

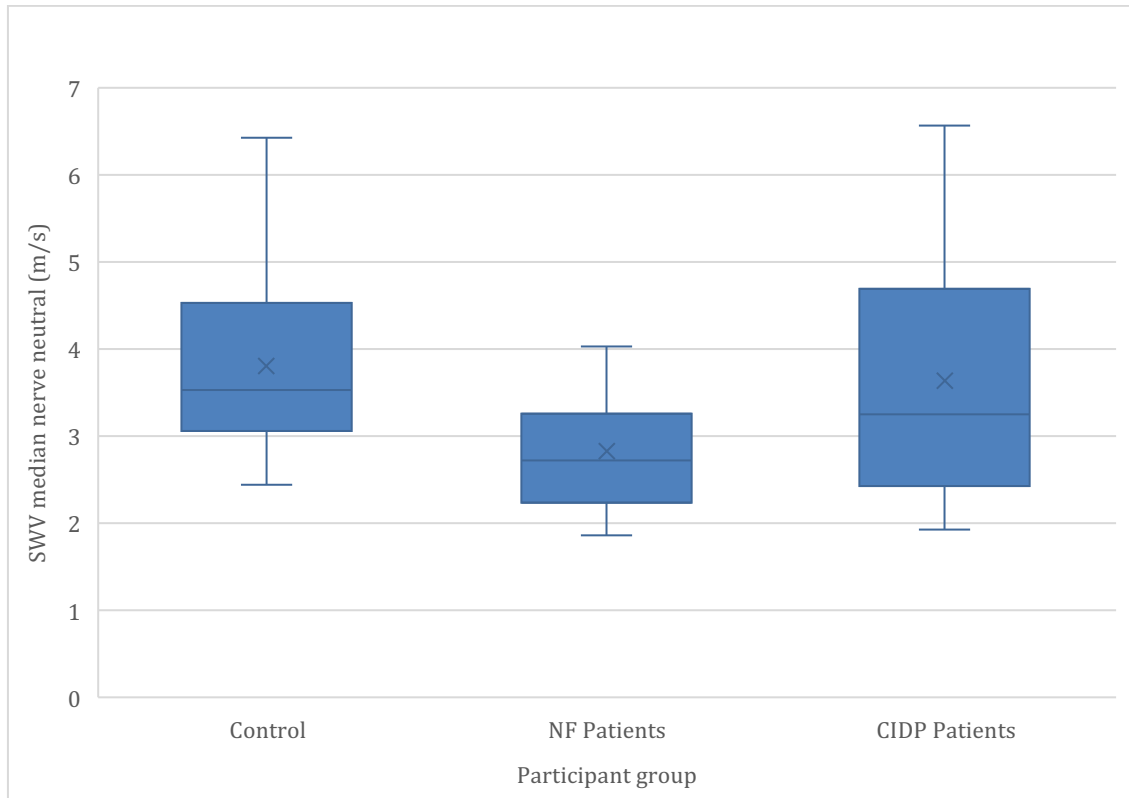


Figure 18. SWV of median nerve with wrist in neutral position in Control, NF and CIDP group. (Own representation) SWV is in m/s.

In conclusion, the neutral wrist position the NF have a lower SWE, the CIDP has a larger range in SWV, and the NF group has the smallest range and variance.

3.5.1.3. SWE in flexion

Lastly, the SWE in flexion was carried out in all three patient groups: Control, NF and CIDP.

Participant Group	Mean SWV (m/s)	SD	Variance	Median	Min.	Max.	Range
Control	3.00	0.92	0.84	2.82	1.80	5.30	3.50
NF	2.60	0.59	0.36	2.51	1.84	3.77	1.93
CIDP	3.12	1.88	3.52	2.48	1.88	7.31	5.43

Table 17. SWV of median nerve in full flexion wrist position in NF, Control and CIDP patient groups. All measurements are in m/s. SD = standard deviation. Min. = minimum. Max. = maximum.

Wrist position	SWV (m/s) comparison of median nerve				
	NF (with outliers) vs. CIDP	NF (without outliers) vs. CIDP	CIDP vs. Control	NF (with outliers) vs. Control	NF (without outliers) vs. Control
Flexion	U = 53.5 <i>p</i> = 0.945	U = 50 <i>p</i> = 0.757	U = 45 <i>p</i> = 0.630	U = 84.5 <i>p</i> = 0.250	U = 66.5 <i>p</i> = 0.156

Table 18. SWV comparison of median nerve across all 3 patient groups in flexion wrist position. 'vs' means versus, 'U' means Mann Whitney U Test., '*p*' means exact significance. Two NF outlier participants had over 100 neurofibromas. Significance was calculated with and without the outliers in comparison.

The results from table 17 and 18 show that in wrist flexion position, there are no significant differences in SWV between NF and CIDP, CIDP and the Control group, or NF and the Control group.

In the fully flexed wrist position, the SWV had a lower mean SWV in all three patient groups than that of the neutral and extended wrist position. The mean SWV of NF group had the lowest SWV (2.60 m/s) when wrist was fully flexed. The CIDP group had the highest range (5.53 m/s) and the highest variance (3.52 m/s). The CIDP group however had a statistical outlier (7.31 m/s) (see figure 19).

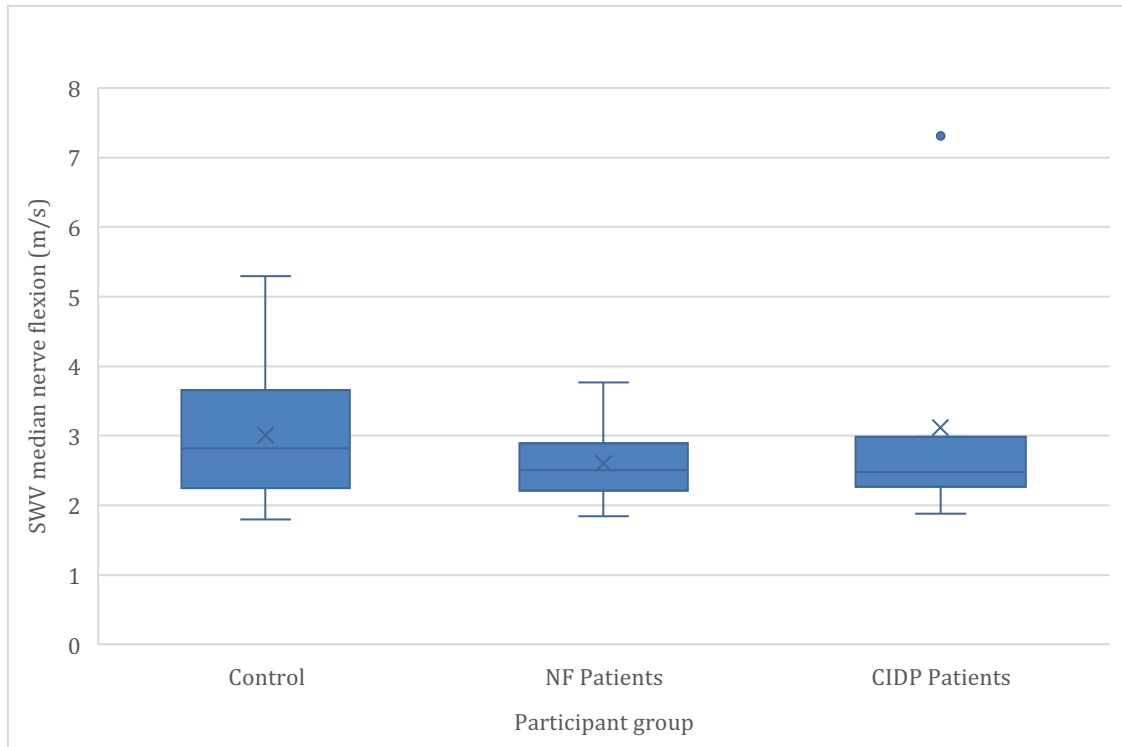


Figure 19. SWV of median nerve with wrist fully flexed in Control, NF and CIDP group. (Own representation) SWV is in m/s.

3.5.2. SWE of forearm and upper arm

To compare whether the nerve had a different elasticity in the forearm compared to the upper arm amongst the three patient groups the SWV was measured in both forearm and upper arm. The NF patient group had their nerve measured in an area where there were no neurofibromas to measure the nerve itself (see table 19).

Participant Group	Median nerve	Mean SWV (m/s)	SD	Variance	Median	Min.	Max.	Range
Control	FA	3.77	1.15	1.32	3.40	2.47	6.54	4.07
NF		3.09	1.14	1.30	2.80	1.64	6.22	4.58
CIDP		3.98	1.79	3.21	3.47	2.29	7.66	5.37
Control	UA	3.38	1.08	1.16	3.14	2.04	6.22	4.18
NF		3.07	1.17	1.38	2.84	1.69	5.9	4.21
CIDP		3.22	0.90	0.81	2.98	2.19	4.80	2.61

Table 19. SWV of median nerve in forearm and upper arm in NF, Control and CIDP patient groups. All measurements are in m/s. Min. = minimum, Max. = maximum. SD = standard deviation. FA = Forearm. UA = Upperarm.

The forearm results showed that the CIDP mean SWV was the highest (3.98 m/s) amongst the three groups, then came the Control group (3.77 m/s) and lastly the NF group (3.09 m/s). The variance was higher for the CIDP patient group (3.21 m/s) while the NF and Control group shared similar variance values (respectively 1.30 m/s and 1.32 m/s). However, without the statistical outliers, the NF group have the lowest range (see table 19 and figure 20).

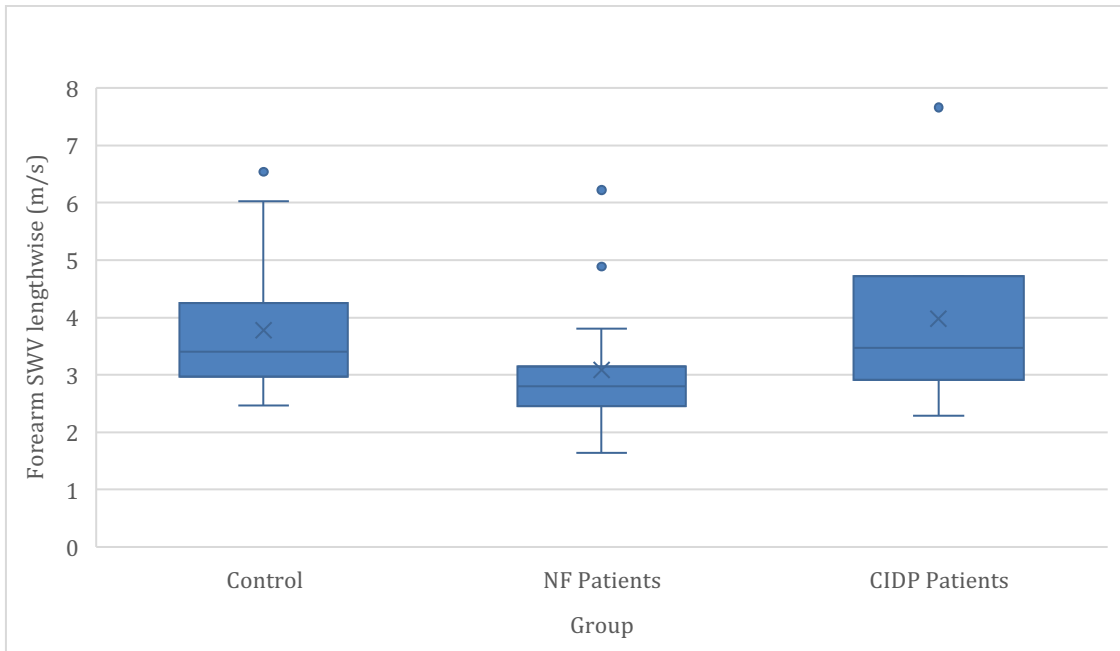


Figure 20. SWV of median nerve in the forearm. (Own representation) SWV is in m/s.

In the forearm, the SWV shows the highest variance in the Control group, and the lowest in the NF group without statistical outliers, however with the outliers included, the variance was highest in the CIDP group, which also had the highest mean SWV (3.98 m/s).

The mean SWV in the upper arm were 3 m/s for Control (3.38 m/s), NF (3.07 m/s) and CIDP (3.22 m/s). the variance was highest in the Control group (1.16 m/s) and lowest for the CIDP group (0.81 m/s (see table 19 and figure 21).

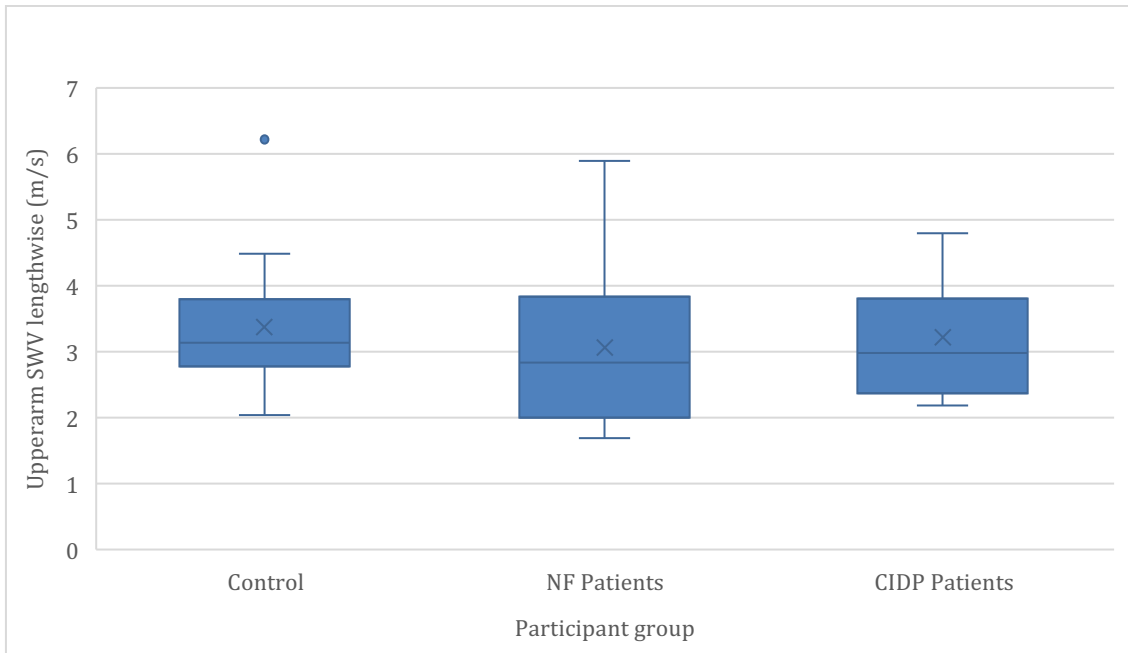


Figure 21. SWV of median nerve in upper arm. (Own representation) SWV is in m/s.

Comparing the forearm with the upper arm in the Control group, the mean SWV decreased from the forearm (3.77 m/s) to in the upper arm (3.38 m/s). The variance also decreased from the forearm (1.32 m/s) to the upper arm (1.16 m/s) while the range rose (4.07 m/s to 4.18 m/s). The NF group also showed the same decrease between the mean SWV mean in the forearm (3.09 m/s) to in the upper arm (3.07m/s) and showed the variance increase (from 1.30 m/s to 1.38 m/s). The CIDP group, also had a SWV decrease from forearm to upper arm (from 3.98 m/s to 3.22 m/s). The variance too showed a decrease in the forearm (3.21 m/s) to the upper arm (0.81 m/s).

According to these results, it can be said that the forearm has a higher SWV than the upper arm in all three patient groups, that the SWV variance is slightly higher in the upper arm for NF and Control group but not for the CIDP group. The variance increases in the upper arm for the CIDP group.

Comparison	With or without outliers	Sig. (<i>p</i>)	Correlation coefficient
SWV (m/s) of median nerve in forearm vs. forearm nerve height (mm)	With outlier	0.174	-0.370
SWV (m/s) of median nerve in forearm vs. forearm nerve width (mm)		0.091	0.137
SWV (m/s) of median nerve in upper arm vs. upper arm nerve height (mm)		0.372	-0.248
SWV (m/s) of median nerve in upper arm vs. upper arm nerve width (mm)		0.398	-0.236
SWV (m/s) of median nerve in forearm vs. forearm nerve height (mm)	Without outlier	0.273	-0.329
SWV (m/s) of median nerve in forearm vs. forearm nerve width (mm)		0.161	-0.413
SWV (m/s) of median nerve in upper arm vs. upper arm nerve height (mm)		0.348	-0.284
SWV (m/s) of median nerve in upper arm vs. upper arm nerve width (mm)		0.285	-0.321

Table 20. Comparison of the SWV (m/s) in the median nerve in the forearm and upper arm versus height and width of the nerve. 'vs' = versus, 'p' = exact significance. Two NF outlier participants had over 100 neurofibromas. Significance was calculated with and without the outliers in comparison.

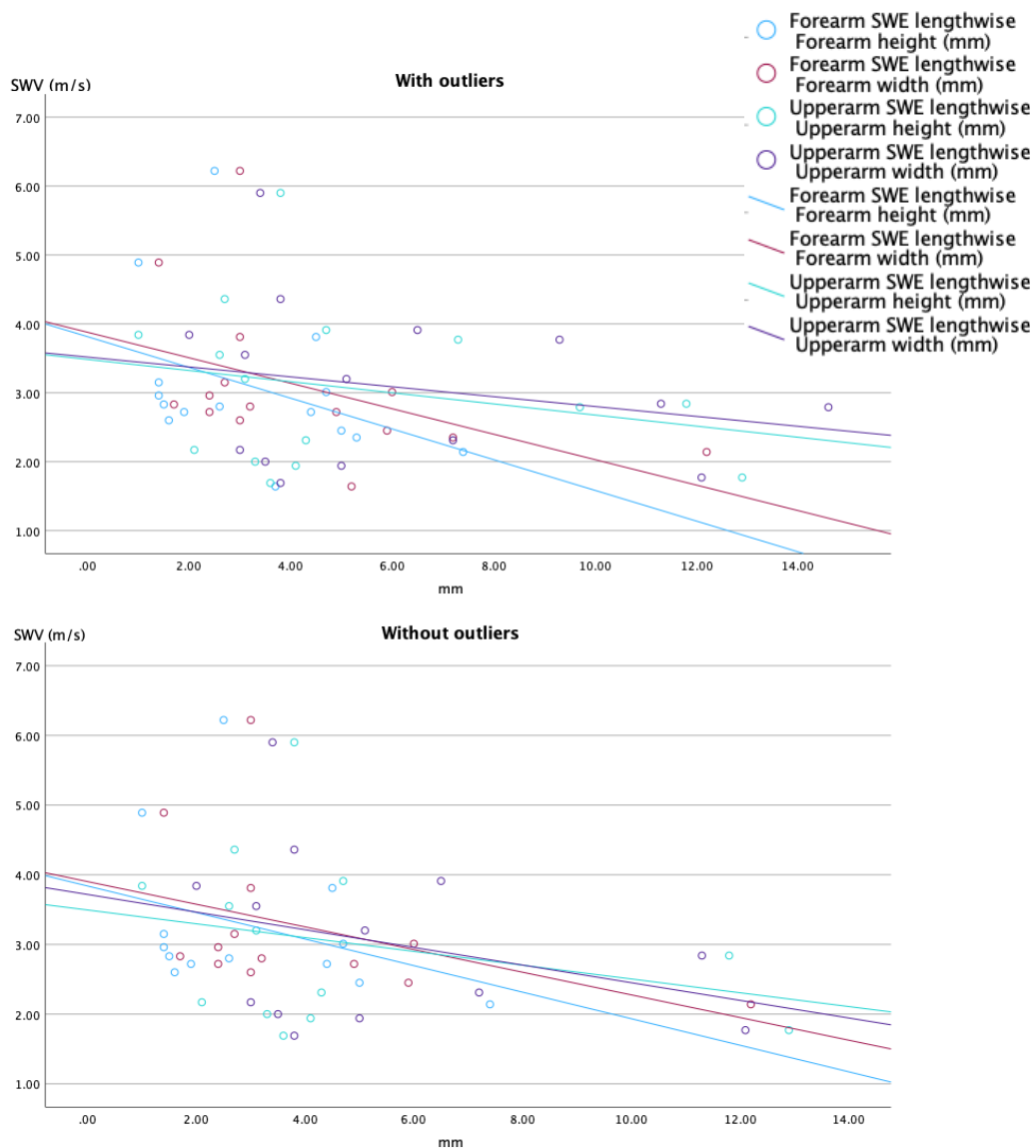


Figure 22. SWV (m/s) of median nerve in forearm and upper arm versus height (mm) and width (mm) of median nerve. The upper graph shows the correlation between the SWV in the forearm and upper arm with all participants while the bottom graph shows the correlation when two outliers with over 200 total neurofibromas each are removed. (Own representation)

The results in table 20 suggest that there is no significant correlation between SWV of the median nerve and the corresponding nerve measurements in the forearm and upper arm, regardless of the presence or absence of NF outliers. Figure 22 offers a visual representation of the correlation in NF patients between SWV (in forearm and upper arm) and the width and height of the median nerve with and without the outliers. Without the outliers, the correlations amongst all comparisons are more similar than with the outliers.

3.5.3. SWV vs. number of neurofibroma in NF patients

The table 21 presents the comparisons between SWV (m/s) of the median nerve and the total number of neurofibromas, considering the presence or absence of outliers. In the "With outlier" group, there was a significant correlation between SWV in extension and the total number of neurofibromas ($p = 0.001$). However, in the "Without outlier" group, the correlation in extension showed a weaker and non-significant trend ($p = 0.055$). The correlations in neutral and flexion positions did not reach statistical significance in both groups. Figure 23 visualises table 21 and shows that without the outliers, SWV in neutral and flexion vs. total numbers of neurofibromas switch from positive to a negative correlation (respectively from 0.011 to -0.268 and 0.070 to -0.254).

Comparison	With or without outliers	Sig. (p)	Correlation coefficient
SWV (m/s) of median nerve in extension vs. total number of neurofibromas	With outlier	0.001	-0.748
SWV (m/s) of median nerve in neutral vs. total number of neurofibromas		0.968	0.011
SWV (m/s) of median nerve in flexion vs. total number of neurofibromas		0.805	0.070
SWV (m/s) of median nerve in extension vs. total number of neurofibromas	Without outlier	0.055	-0.542
SWV (m/s) of median nerve in neutral vs. total number of neurofibromas		0.376	-0.268
SWV (m/s) of median nerve in flexion vs. total number of neurofibromas		0.401	-0.254

Table 21. Comparison of the SWV (m/s) in the median nerve in extension, neutral and flexion wrist position vs total number of neurofibromas. 'vs' means versus, ' p ' means exact significance. Two NF outlier participants had over 100 neurofibromas. Significance was calculated with and without the outliers in comparisons. Significance in bold are significant.

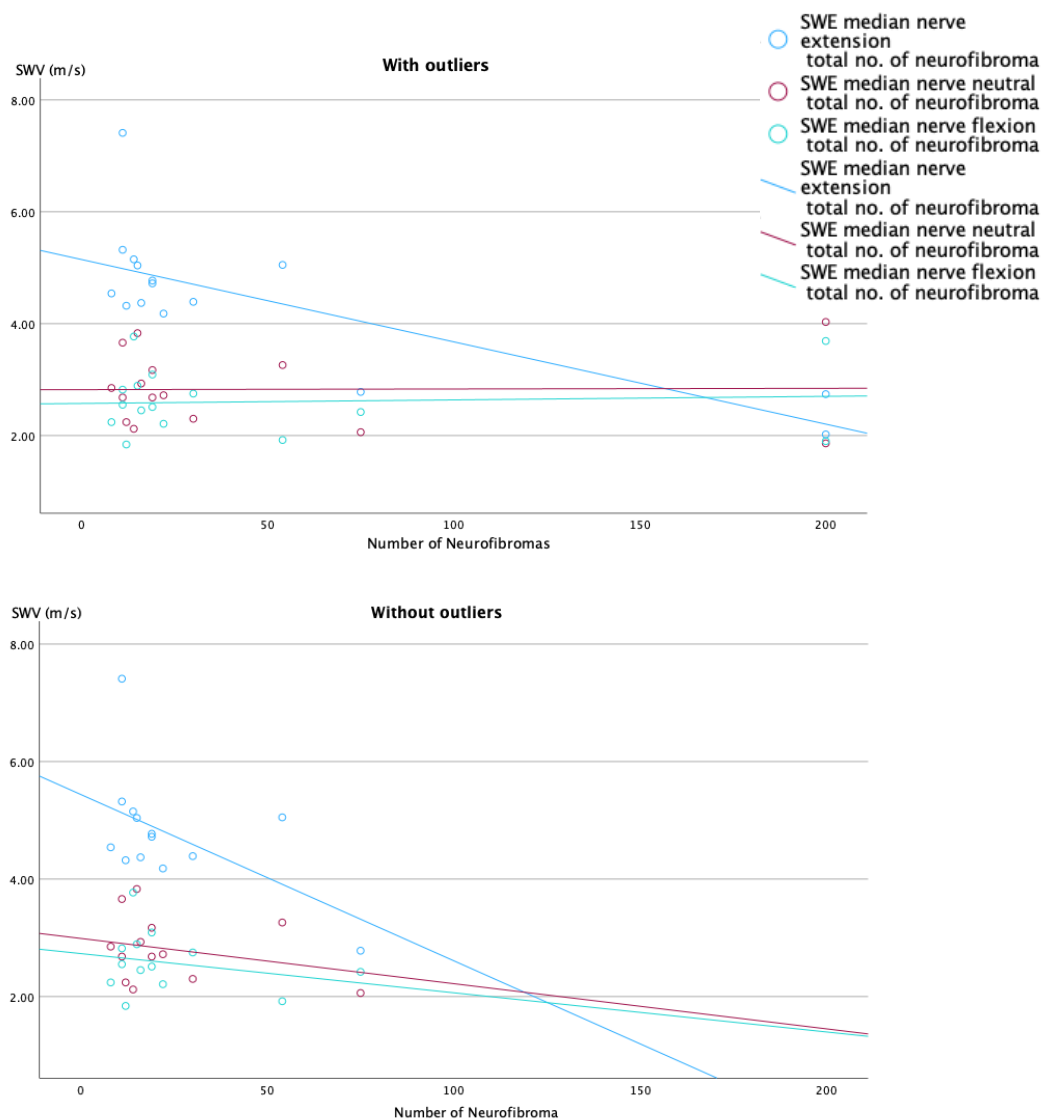


Figure 23. SWV (m/s) of median nerve in forearm with wrist in extension, neutral and flexion. Upper graph shows the correlation between the SWV in the three wrist positions with all participants while the bottom graph shows the correlation when two outliers with over 200 total neurofibromas are removed. (Own representation)

4. Discussion

This thesis tested whether SWE could be implemented on enlarged nerves and whether it was possible to differentiate between two causes of enlarged nerves- inflammation and tumours.

4.1. NF

Investigating the SWE of PNTs in neurofibromatosis takes a first step towards describing the elasticity of benign PNTs and their potential biomechanical influence on peripheral nerves (Staber et al., 2022). Due to the benign tumour entity and the homogenous ultrasound characteristics of neurofibromas and schwannomas (Jacques and Dietemann, 2005) (Staber et al., 2022), NF can be regarded as a model disease to explore the potential of SWE for PNTs (Staber et al., 2022).

As there are no SWE studies on PNTs, a comparison to benign tumours out with nerves was needed (Staber et al., 2022). PNTs in this thesis exhibited an average SWV of 2.82 m/s, with the matched controls having a higher SWV average of 3.81 m/s (Staber et al., 2022). In comparison, another study measured the SWV of 57 parathyroid adenomas and obtained a mean SWV of 2.02 m/s (Azizi et al., 2016) (Staber et al., 2022), compared to a healthy unaffected thyroid parenchyma higher SWV value of 2.77 m/s. In these cases, healthy parathyroid adenomas, and healthy median nerves both have higher SWV than that of their pathological counterpart.

Why adenomas for comparison? Like PNTs, adenomas are identified as predominantly dense and having a solid body (Staber et al., 2022). However, unlike PNTs, adenomas are described as without a clear boundary (Kuo et al., 2020) (Staber et al., 2022). PNT boundaries are rather unmistakable with ultrasound (Staber et al., 2022). Although similar in some respects and different in other respects, adenomas and PNTs could be used for comparison with SWV (Staber et al., 2022). This comparison would show that the PNTs have a faster SWV of just under 50% than the SWV of adenomas (Staber et al., 2022). This difference could be hypothetically due to certain characteristics, such as the hard-to-define boundaries of the adenomas, i.e., healthy tissue could be potentially included in the measurement, which would affect the SWV (Staber et al., 2022). When comparing Control and NF nerve the mean values did not deviate too much (see Table 12) as the NF patients were matched with control patients of similar

BMI and age. Naturally slight differences could not be avoided due to the given time frame to find suitable matching controls which agreed to participate.

Comparing the PNTs SWV with existing literature was challenging due to there being no studies for SWE on PNTs. While adenomas seems like a feasible comparison, one can also use other body tissues to identify the relationship between healthy and pathological tissue with SWE. Liu et al. (Liu et al., 2019) used SWV for the differentiation of tumours of the cervix uteri, with a mean of 3.53 m/s among 40 patients with benign tumours and 2.86 m/s in the Control group, while the 138 patients with malignant tumours showed higher mean SWV at 4.91 m/s (Staber et al., 2022). Again, unlike the PNTs, the cervical carcinomas have unclear boundaries as well as an irregular shape which should be taken into consideration when comparing the trend between healthy and pathological tissue between PNTs and adenomas (Staber et al., 2022). Regarding further studies differentiating benign and malignant tumours with ultrasound SWE, Ozturk et al. (Ozturk et al., 2020) (Staber et al., 2022) and Zhong (Zhong et al., 2021) investigated SWE in breast lesions (Staber et al., 2022). Benign breast lesions showed a mean SWV of 3.30 m/s, whereas malignant lesions had a lower mean SWV of 2.87 m/s (Ozturk et al., 2020) (Staber et al., 2022). Here, the two studies contradict as to whether the malignant tissue has a higher SWV or not.

Not only can the SWE be calculated and compared in healthy and pathological tissue, but it can also observe how the SWE of the measured tissue changes in different situations such as positioning of limbs and how this changes the stiffness. One can presume that the “stiffer” the nerve, the higher the estimated SWV (Staber et al., 2022). For example, in CTS patients showed an increased mean SWV in comparison to the HC (Kantarci et al., 2014) (Staber et al., 2022). In line with other SWE-studies about the median nerve, the SWV of the median nerve in neutral position in HC was 3.8 m/s; other studies report SWV between 3.1– 4.0 m/s (Zhu et al., 2018) (Staber et al., 2022). Interestingly, the SWV of the median nerve in NF patients showed a lower SWV (2.8 m/s) in neutral position (Staber et al., 2022). This difference was even more evident when comparing

different wrist joint positions (Staber et al., 2022). With and without the NF outliers, there was a significant difference ($p = 0.004$ and $p = 0.002$) in SWV when wrist was in neutral position when comparing NF and Control which indicates potential abnormalities in nerve conduction in individuals with NF (Staber et al., 2022). This also allows for a differentiation of SWV between an NF nerve and a Control nerve.

When the wrist joint is fully extended, the muscles around the median nerve are tensed while the nerve is also stretched due to the extension, resulting in higher compression of the nerve (Zhu et al., 2018) (Greening and Dilley, 2017) (Rugel et al., 2020) (Staber et al., 2022). There was a significant difference in SWV in both NF groups and the Control group with ($p = 0.019$) and without outliers ($p = 0.01$) suggesting that SWE could be used to differentiate between NF and healthy median nerves in extended wrist position.

When the wrist joint is fully flexed, relaxing the muscles around the nerve, creating less compression (Staber et al., 2022). There were no significant differences in SWV between NF and the Control group which may be due to the small sample sizes. The pathological nerve of the NF patients had a mean SWV of 2.8 m/s, meaning that the median nerves of the NF patients were less “stiff” (Staber et al., 2022). Therefore, a pathological nerve may lead to a differing biomechanical effect depending on the pathology (Staber et al., 2022). Further, influence of PNTs on the general stiffness of the nerve is possible (Staber et al., 2022). The stiffness of the median nerve differs depending on the position in the wrist, since the nerve is more under tension in extension than in flexion (Staber et al., 2022). We were able to confirm this in our measurements in healthy subjects (Staber et al., 2022). Thus, there was a higher stiffness in extension than in flexion or in neutral zero position (Staber et al., 2022). However, since SWE is still relatively young in the neurological field, more research with larger patient groups is recommended (Staber et al., 2022).

In our study, patients with PNTs showed lower values than the Controls when SWE of the median nerve was measured in the same position in extension and flexion (Staber et al., 2022). Thus, neurofibromas appear to influence the stiffness of the nerve when the nerve is stretched (Staber et al., 2022). Andrade et al. used the ankle and knee positioning of healthy participants to study whether the SWE was affected and came to the conclusion that the SWV increased with ankle in dorsiflexion when the knee was extended and that the SWV decreased throughout five repeated ankle rotation motions (Andrade et al., 2016).

One possible hypothesis is that PNTs have a similar effect as that of a pulley used in a block and tackle: when the nerve is stretched, the stretching force will be reduced by the neurofibroma, acting as a pulley (Staber et al., 2022). Consequently, the force due to the stretching will be reduced and hence also the “stiffness”, i.e., the SWV will be reduced (Staber et al., 2022). According to this hypothesis, the number of neurofibromas (or simply speaking, the number of pulleys) in the nerve should correlate with the SWV (Staber et al., 2022). In our small sample of 15 NF patients, we found a trend that the number of PNTs correlated negatively with the SWV, but we consider this correlation not representative due to the small sample size (Staber et al., 2022). Here, studies with larger sample sizes are needed (Staber et al., 2022). Larger sample sizes could not be achieved as the patient recruitment took place in the corona virus pandemic which made patients wary of coming into the hospital where there were patients with COVID-19. As the disease is also rare many patients lived far away, too far away to be prepared to come to Tübingen for a study that takes under one hour. Transportation costs were also not covered. This results in the limited sample sizes.

Whether or not the mean calculated SWV lies on the lower end of the spectrum, or the higher end is still questionable, as there are simply not enough large-scale SWE studies in benign homogenous tumours to facilitate comparison (Staber et al., 2022). Amongst the above-mentioned studies, the NF mean SWV tends to run a little slower in comparison to other benign tumours (Staber et al., 2022).

Further studies are needed to assess if ultrasound SWE can also be utilised to differentiate between benign and malignant tumours in peripheral nerves (Staber et al., 2022). This thesis' results encourage such studies, as it shows that the benign nerve tumour entities neurofibromas and schwannomas are in a similar range as other benign tumours (Staber et al., 2022). Consequently, it seems likely that malignant nerve tumours might also have—comparable to malignant non-nerve tumours—a higher SWV (Staber et al., 2022).

4.2. CIDP

Having discussed whether SWE works for NF, the same must be discussed for the other chosen model disease, CIDP. While it is known and well-practiced to use ultrasound for CIDP patients, there are no studies using SWE for CIDP.

CIDP is a well suited counterplayer for NF to explore whether SWE can differentiate between enlarged nerves due to inflammation or tumours. Unlike the focal neoplastic nerve enlargement in NF, the CIDP patients have a proximal emphasis of nerve thickening which is stretched long throughout the nerve as a hypertrophic neuropathy (Lehmann et al., 2019). As CIDP is an inflammatory polyneuropathy, it is known that the surrounding tissue becomes stiffer due to the ongoing inflammatory process in the nerve (Osterman et al., 2014). It can be therefore presumed that the nerve itself becomes stiffer which can be also felt as a thicker and harder nerve. CIDP is, like NF, also a rare disease and the same applies to CIDP as it did with NF regarding small sample sizes. It was very difficult to obtain a large patient group due to the pandemic situation. Additionally, patients with a larger UPSS were selected, and from these patients those that did not have a known UPSS of the median nerve were not included in the patient group. This shrunk the patient group size considerably. Amongst all three participant groups, CIDP had the highest mean age of 68 years old due to the late average onset of disease at 50 years old (Dimachkie and Barohn, 2013). UPSS was not calculated for this thesis, however, it had already been calculated and stated in the patient data. The UPSS value for the median nerve was also generalised and not specific for forearm and upper arm. This could lead to

different values as, already mentioned, the CIDP shows an emphasis proximally which could result in different UPSS values for forearm and upper arm.

SWE works on CIDP; however, it cannot be used to accurately differentiate between NF, the PNT, and CIDP, the inflammation. Using the Mann-Whitney U test there were no significant results to be able to differentiate between NF and CIDP. To make sure these results are not due to small sample groups, much higher sample numbers are needed for follow-up studies. The aim was to explore whether it could be used to differentiate different causes for nerve enlargement, tumours, or inflammation. As this had never been investigated before, it was important to have explored this option as this could further the diagnostic and monitoring of pre-existing and future CIDP patients. While it is proven that ultrasound works for CIDP (Bunschoten et al., 2019), SWE can be used to some extent in combination with other diagnostic tools such as lumbar puncture or even nerve biopsy (Eftimov et al., 2020).

Comparing CIDP to other similar conditions such as AIDP allows for an understanding of how a similar nerve pathology may differ or share similarities. With these comparisons, (Zaidman and Pestronk, 2014b) assumptions or even relationships can be made more easily for other diseases in monitoring, diagnostic or therapy which would affect another patient group out with CIDP or NF.

By using ultrasound, Zaidmann et al. also examined peripheral nerve size in patients with polyneuropathy using ultrasound (Zaidman et al., 2009). While they didn't use SWE, their patient demographic results can be used to compare whether the CIDP patient corresponded with our CIDP patient data as our sample size was small. Their adult Control patients had a mean age of 44 years old and a mean BMI of 26 kg/m². Our Control participants had a mean age of 35.9 years and a mean BMI of 26.2 kg/m². To enable comparisons across patients of varying heights, a "nerve size index" can be calculated by adjusting size measurements based on height (Zaidman and Pestronk, 2014b). With an enlarged mean nerve

size indexes of 197, 268 and 136 in the median nerve in the forearm, arm, and wrist for their CIDP patients compared to their Control patients nerve size indexes at 93, 110 and 100 and AIDP at 118, 159 and 138, the nerve enlargement neuropathies did show an enlarged nerve. This increase in nerve enlargement can be seen in this thesis. While nerve size indexes were not used the median nerve height and width were measured using ultrasound. The Control patients had a mean height of the median nerve in the forearm of 3.1 mm and width of 4.6 mm while the CIDP patients had a mean height and width of 3.9 mm and 6.7 mm. Here too, the CIDP showed a larger height and width which would translate to a larger nerve size index.

Using the CIDP patient group, the biomechanical effect was measured on a pathological nerve. This was not possible in the NF patient group as it is assumed that the NF patient group have PNTs throughout the physiological nerve whereas the CIDP patients have a pathological nerve (without PNTs of course).

The biomechanical effect was measured in the wrist joint due to practicality. The nerve thickening in CIDP is predominately proximal emphasised (Koike and Katsuno, 2020). To test the biomechanical effect of the upper arm, it would have been highly uncomfortable for the patients as well as physically difficult for patients according to age and agility. Therefore, the biomechanical effect was tested in the wrist joint as it can assumed that most patients, regardless of age or agility can perform a maximum flexion and extension in the wrist joint. The CIDP group were compared to the NF group and Control group as a pathological nerve. Note that the median nerve of the patient with a NF diagnosis was measured where there were no NF tumours. Participants were not questioned whether they were medicated with immunoglobulins or any other medication which could suppress the chronic nerve infection which could decrease the nerve thickness (Castle and Robertson, 2019). This may alter the biomechanical effect for the pathological nerve. Nor was asked how long the patients knew of their diagnosis.

There is no research regarding the biomechanical effect of the median nerve during different wrist positions in CIDP using SWE. However, Rugel et al. had conducted a similar study showing that in extension the SWV was higher in extension than flexion in the healthy median nerve (Rugel et al., 2020). This was the case for both in proximal and distal parts of the nerve which mirror what the Controls, the NF and the CIDP patients showed in our study. Interestingly, the Rugel et al study also found that the ulnar nerve had a greater SWV proximally for both flexion and extension while the median nerve did not. This would be interesting to know whether this was the case for the CIDP patients since the disease is largely proximally emphasised.

4.3. Ultrasound SWE

While SWE has many advantages, there are limitations to SWE. These limitations, which can prove to be difficult to control and therefore affect results can be categorised into two groups: external and internal (see Table 22).

External factors	Internal factors
Volume of gel used	Tissue pennation angle
Examiner skill	BMI (kg/m ²)
Pre-load	Age (years)
Depth of SWE	Joint Position
Ultrasound system	Sex
Ultrasound transducer	Anisotropy
Plane of transducer	
Plane	

Table 22. A summary of the external and internal factors which can influence ultrasound SWE calculations.

External limitations of SWE are limitations which are not related to the patient. This can include the examiner [14] (Gennisson et al., 2013) or even the examination device. Not only are there differences amongst examiners (inter-

examiner differences), but there are also intra-examiner differences which can affect the SWE. When the transducer is pressed onto the skin upon contact, the pressure, or also known as pre-load, can vary affecting the obtained SWE values from the examiner. More pre-load means higher pressure carried out on the underlying tissue causing an increased elasticity value (Carpenter et al., 2015). This increase in elasticity is due to the caused compression on the underlying tissue. If the muscle is compressed a nearby nerve may also be compressed too. This has not been proven yet in nerves. It is difficult to quantify the pre-load pressure subjectively in intra- and inter examiner examinations and therefore considered the main limitation of SWE (Gennisson et al., 2013). It is debated that in order to prevent this limitation from becoming too dominant, there should be no contortion of the tissue under the transducer therefore minimising the pre-load (Alfuraih et al., 2018) (Correas et al., 2013) (Cortez et al., 2016) (Hall et al., 2013).

Naturally, the volume of ultrasound gel can vary between patients as some patients may need more than others, as well as between inter- and intra-examiner examinations which also can affect the SWE values obtained. This has been proven to be the case in SWE studies of breast and thyroid tissue (Barr and Zhang, 2012) (Lam et al., 2016). The company Standoff gel claims that by applying 5mm of ultrasound gel onto the skin, the transducer will not deform the gel (Alfuraih et al., 2018). Additionally, little air bubbles that occur within the gel can also affect the push-pulse emitted from the transducer. This can result in a larger variance as well as a lower reliability. Some studies point out that if a larger volume of ultrasound gel is used in combination with minimal pressure, then errors can be avoided (Cortez et al., 2016). To date, there is no recommended or standardised volume of gel to be used when performing SWE.

Like ultrasound, SWE is also limited by the depth of the selected tissue from the transducer when in contact with the tissue surface (Taljanovic et al., 2017). The median nerve does not run completely superficial like other structures such as muscles. Other nerves or tumours may lie too deep for the SWV to be measured accurately (Alfuraih et al., 2018), out with the reach of the transducer. While some

studies (Alfuraih et al., 2018) prove that more superficial the structure or interest the higher the reliability of the SWE results, there are other studies (Carpenter et al., 2015) (Ewertsen et al., 2016) that argue about how depth affects the SWE results. While there is not a recommended SWE variability for nerves, the thyroid SWE for example, should not be taken at a depth over 5cm (Cosgrove et al., 2012).

The device itself also entails external factors as there are various software which can be purchased which provide SWE. Even amongst the same software, there are various settings from which can be chosen to the examiners liking. Such settings include ROI size (region of interest) (Alfuraih et al., 2017) (Ewertsen et al., 2016). A difference in settings or in software may affect SWE. Depending on what tissue is of interest, there are different transducer types which are best suited for certain tissues, or body parts or expertise which may result in different values.

Whether the same examiner, or different examiners use the transducer on the same patient can be seen as an external factor. Some studies, have proven to have inter- as well as intra-examiner reliability in SWE. This is calculated by using the ICC (intraclass correlation coefficient) which simply measures in test-retest inter- and intra-examiner situations (Cortez et al., 2016) (Chino et al., 2014). The higher the reliability, the higher the ICC value (Koo and Li, 2016). Values below 0.5 are considered poor, from 0.5 to 0.75 considered as moderate, from 0.75 to 0.9 are good while 0.9 and above are excellent.

As mentioned above, there are also internal limitations to SWE. One being the anisotropic nature of the tissue being measured. This means that the tissue being measured is not completely homogenous and possibly contains different properties and compositions. The more anisotropy, the higher the SWV and the less reliable SWV results. In body tissue, this can take the form of blood vessels, calcifications and microlesions for example. Healthy nerve tissue can be considered relatively homogenous, in comparison to muscle tissue. Different types of tissue within the measured tissue can alter the SWV measured. A

relevant nerve tissue abnormality is calcifications which affect SWE values. Amongst NF patients, calcifications were found when measuring SWV of patients in this thesis. To minimise the anisotropy, the transducer can be positioned mirroring the longitudinal plane of the tissue fibres (Alfuraih et al., 2017) (Eby et al., 2013) (Gennisson et al., 2013).

It was proven that the joint position can affect SWE results in muscles (Berrigan et al., 2020) (Boulard et al., 2021). The biceps brachii muscle shear modulus was significantly higher ($p < 0.0001$) in maximum extension compared to when elbow in 90° , which would indicate that the muscle was tensed in extension and therefore compressing the median nerve to some extent (Eby et al., 2013). Interestingly, both the extension and the flexion were passive. This would show that even a passive joint change causes changes in SWE as the nerve surrounding tissue can impact the shear modulus of the nerve.

On the one hand, observations were made that patients with a higher BMI had a higher SWE in almost all muscles since there would be a greater anatomical pre-load. On the other hand, it has also been proven that there is no clear correlation between increased BMI and higher SWE (Tang et al., 2020) (Alfuraih et al., 2019). This could then be the case with the nerves, e.g., the median nerve, which are also affected by the surrounding increase in pressure from the surrounding fat tissue causing the increase in BMI. However, Bedewi et al. showed that the SWE of the saphenous nerve showed no correlation with BMI, age, height and weight (Bedewi et al., 2020.). Nonetheless, the BMI and age should be considered in further studies as nerve can differ in location and situation (Ishibashi et al., 2016) (Creze et al., 2018). This is because the age of the patient correlates with the fat depot distribution which naturally occurs with ageing (Kuk et al., 2009). Older patients experience a gradual fat redistribution from the abdominal-visceral/gluteal-femoral region to muscle and beneath its fascia (subcutaneous fat storage) (Sepe et al., 2011).

5. Summary

5.1. English Summary

This thesis shows that the SWE measurement of PNTs is feasible and as previous studies with other benign tumours, aside from PNTs, also showed to have a low SWV. Furthermore, we speculate that the presence of PNTs may have a biomechanical impact on peripheral nerves that has not yet been demonstrated (Staber et al., 2022).

The hypothesis that there is a significant difference between NF and CIDP SWE proved to be wrong. The second hypotheses that the neurofibroma alter the shear wave velocity (SWV) during different biomechanical positions of the median nerve (in our case throughout the wrist joint: zero-degree, maximal flexion, and maximal extension) proved to be correct (Staber et al., 2022). The mean SWV in extension for NF was lower (4.5 m/s) than that of Control (5.8 m/s), lower in neutral (2.8 m/s) compared to the Control (3.8 m/s) and again lower in flexion (2.6 m/s) than that of the Control (3 m/s).

The SWE of enlarged nerves, due to tumours or inflammation, has been proven to be possible, while a clear differentiation using SWE between NF and CIDP remains difficult. Analysis of biomechanical effects can be undergone but should entail standardised protocols and with attention to the limitations that come with SWE. Larger patient groups are needed for an accurate representation of the patient groups to determine whether SWE can differentiate between NF and CIDP and healthy nerves.

Nonetheless, SWE shows a promising future within neurology departments thanks to its cheap and flexible usage and will undoubtedly prove to be of more importance in the upcoming years as a comparably new non-invasive technology.

5.2. German Summary - Deutsche Zusammenfassung

Diese Arbeit zeigt, dass die Messung von PNTs machbar ist und ein niedriges SWV aufweist, dass auch anderen gutartigen, nicht nerven Tumoren ähnelt.

Darüber hinaus spekulieren wir, dass das Vorhandensein von PNTs einen biomechanischen Einfluss auf periphere Nerven haben könnte, der bisher noch nicht nachgewiesen wurde.

Die Hypothese, dass es einen signifikanten Unterschied zwischen NF und CIDP SWE gibt, hat sich als falsch erwiesen. Die zweite Hypothese, dass das Neurofibrom die Scherwellengeschwindigkeit (SWV) in verschiedenen biomechanischen Positionen des Nervus Medianus (in unserem Fall im gesamten Handgelenk: Null-Grad, maximale Flexion und maximale Extension) verändert, erwies sich als richtig: Die mittlere SWV in Extension war bei NF niedriger (4,5 m/s) als bei der Kontrolle (5,8 m/s), niedriger in der Neutralstellung (2,8 m/s) im Vergleich zur Kontrolle (3,8 m/s) und wiederum niedriger in der Flexion (2,6 m/s) als bei der Kontrolle (3 m/s).

Die SWE vergrößerter Nerven aufgrund von Tumoren oder Entzündungen ist nachweislich möglich, während eine eindeutige Differenzierung zwischen NF und CIDP anhand der SWE schwierig bleibt. Eine Analyse der biomechanischen Effekte ist möglich, sollte aber mit standardisierten Protokollen und unter Berücksichtigung der mit der SWE verbundenen Einschränkungen erfolgen. Um festzustellen, ob die SWE zwischen NF und CIDP unterscheiden kann, sind größere Patientengruppen erforderlich, um eine genaue Repräsentation der Patientengruppen zu erreichen.

Nichtsdestotrotz hat die SWE dank ihrer kostengünstigen und flexiblen Anwendung eine vielversprechende Zukunft in den neurologischen Abteilungen und wird in den kommenden Jahren zweifellos an Bedeutung gewinnen, da es sich um eine verhältnismäßig neue nicht-invasive Technologie handelt.

6. References

- Ageeli, W., Wei, C., Zhang, X., Szewczyk-Bieda, M., Wilson, J., Li, C., Nabi, G., 2021. Quantitative ultrasound shear wave elastography (USWE)-measured tissue stiffness correlates with PIRADS scoring of MRI and Gleason score on whole-mount histopathology of prostate cancer: implications for ultrasound image-guided targeting approach. *Insights Imaging* 12, 96. <https://doi.org/10.1186/s13244-021-01039-w>
- Akagi, R., Kusama, S., 2015. Comparison Between Neck and Shoulder Stiffness Determined by Shear Wave Ultrasound Elastography and a Muscle Hardness Meter. *Ultrasound Med. Biol.* 41, 2266–2271. <https://doi.org/10.1016/j.ultrasmedbio.2015.04.001>
- Alfuraih, A.M., O'Connor, P., Hensor, E., Tan, A.L., Emery, P., Wakefield, R.J., 2018. The effect of unit, depth, and probe load on the reliability of muscle shear wave elastography: Variables affecting reliability of SWE. *J. Clin. Ultrasound JCU* 46, 108–115. <https://doi.org/10.1002/jcu.22534>
- Alfuraih, A.M., O'Connor, P., Tan, A.L., Hensor, E., Emery, P., Wakefield, R.J., 2017. An investigation into the variability between different shear wave elastography systems in muscle. *Med. Ultrason.* 19, 392. <https://doi.org/10.11152/mu-1113>
- Alfuraih, A.M., Tan, A.L., O'Connor, P., Emery, P., Wakefield, R.J., 2019. The effect of ageing on shear wave elastography muscle stiffness in adults. *Aging Clin. Exp. Res.* 31, 1755–1763. <https://doi.org/10.1007/s40520-019-01139-0>
- Andrade, R.J., Nordez, A., Hug, F., Ates, F., Coppieters, M.W., Pezarat-Correia, P., Freitas, S.R., 2016. Non-invasive assessment of sciatic nerve stiffness during human ankle motion using ultrasound shear wave elastography. *J. Biomech.* 49, 326–331. <https://doi.org/10.1016/j.jbiomech.2015.12.017>
- Antinheimo, J., Haapasalo, H., Seppälä, M., Sainio, M., Carpen, O., Jääskeläinen, J., 1995. Proliferative potential of sporadic and neurofibromatosis 2-associated schwannomas as studied by MIB-1 (Ki-67) and PCNA labeling. *J. Neuropathol. Exp. Neurol.* 54, 776–782. <https://doi.org/10.1097/00005072-199511000-00004>
- Antoniolli, L.P., Milman, L. de M., Bonamigo, R.R., 2021. Dermoscopy of the iris: identification of Lisch nodules and contribution to the diagnosis of Neurofibromatosis type 1. *An. Bras. Dermatol.* 96, 487–489. <https://doi.org/10.1016/j.abd.2020.09.007>
- Azizi, G., Piper, K., Keller, J.M., Mayo, M.L., Puett, D., Earp, K.M., Malchoff, C.D., 2016. Shear wave elastography and parathyroid adenoma: A new tool for diagnosing parathyroid adenomas. *Eur. J. Radiol.* 85, 1586–1593. <https://doi.org/10.1016/j.ejrad.2016.06.009>
- Barr, R.G., 2015. WFUMB Guidelines and Recommendations for Clinical Use of Ultrasound Elastography: Part 2: Breast. *Ultrasound Med. Biol.* 41, 13.
- Barr, R.G., Nakashima, K., Amy, D., Cosgrove, D., Farrokh, A., Schafer, F., Bamber, J.C., Castera, L., Choi, B.I., Chou, Y.-H., Dietrich, C.F., Ding,

- H., Ferraioli, G., Filice, C., Friedrich-Rust, M., Hall, T.J., Nightingale, K.R., Palmeri, M.L., Shiina, T., Suzuki, S., Sporea, I., Wilson, S., Kudo, M., 2015. WFUMB Guidelines and Recommendations for Clinical Use of Ultrasound Elastography: Part 2: Breast. *Ultrasound Med. Biol.* 41, 1148–1160. <https://doi.org/10.1016/j.ultrasmedbio.2015.03.008>
- Barr, R.G., Zhang, Z., 2012. Effects of precompression on elasticity imaging of the breast: development of a clinically useful semiquantitative method of precompression assessment. *J. Ultrasound Med. Off. J. Am. Inst. Ultrasound Med.* 31, 895–902. <https://doi.org/10.7863/jum.2012.31.6.895>
- Battaglia, P.J., Carbone-Hobbs, V., Guebert, G.M., Mackinnon, S.E., Kettner, N.W., 2017. High-resolution ultrasonography and shear-wave sonoelastography of a cystic radial nerve Schwannoma. *J. Ultrasound* 20, 261–266. <https://doi.org/10.1007/s40477-017-0254-5>
- Berrigan, W.A., Wickstrom, J., Farrell, M., Alter, K., 2020. Hip position influences shear wave elastography measurements of the hamstring muscles in healthy subjects. *J. Biomech.* 109, 109930. <https://doi.org/10.1016/j.jbiomech.2020.109930>
- Blank, P.M.K. de, Fisher, M.J., Liu, G.T., Gutmann, D.H., Listernick, R., Ferner, R.E., Avery, R.A., 2017. Optic Pathway Gliomas in Neurofibromatosis Type 1: An Update: Surveillance, Treatment Indications, and Biomarkers of Vision. *J. Neuro-Ophthalmol. Off. J. North Am. Neuro-Ophthalmol. Soc.* 37, S23. <https://doi.org/10.1097/WNO.0000000000000550>
- Bouillard, K., Nordez, A., Hug, F., 2011. Estimation of Individual Muscle Force Using Elastography. *PLOS ONE* 6, e29261. <https://doi.org/10.1371/journal.pone.0029261>
- Bouirig, K., Cherkaoui, L. ouafae, 2022. Nodules de Lisch: marqueur ophtalmologique de la neurofibromatose de type 1. *Pan Afr. Med. J.* 42, 108. <https://doi.org/10.11604/pamj.2022.42.108.35079>
- Boulard, C., Gautheron, V., Lapole, T., 2021. Mechanical properties of ankle joint and gastrocnemius muscle in spastic children with unilateral cerebral palsy measured with shear wave elastography. *J. Biomech.* 124, 110502. <https://doi.org/10.1016/j.jbiomech.2021.110502>
- Boyd, K.P., Korf, B.R., Theos, A., 2009. Neurofibromatosis type 1. *J. Am. Acad. Dermatol.* 61, 1–16. <https://doi.org/10.1016/j.jaad.2008.12.051>
- Broers, M.C., Bunschoten, C., Nieboer, D., Lingsma, H.F., Jacobs, B.C., 2019. Incidence and Prevalence of Chronic Inflammatory Demyelinating Polyradiculoneuropathy: A Systematic Review and Meta-Analysis. *Neuroepidemiology* 52, 161–172. <https://doi.org/10.1159/000494291>
- Bunschoten, C., Jacobs, B.C., Van den Bergh, P.Y.K., Cornblath, D.R., van Doorn, P.A., 2019. Progress in diagnosis and treatment of chronic inflammatory demyelinating polyradiculoneuropathy. *Lancet Neurol.* 18, 784–794. [https://doi.org/10.1016/S1474-4422\(19\)30144-9](https://doi.org/10.1016/S1474-4422(19)30144-9)
- Campbell, S., 2013. A Short History of Sonography in Obstetrics and Gynaecology. *Facts Views Vis. ObGyn* 5, 213–229.
- Campen, C.J., Gutmann, D.H., 2018. Optic Pathway Gliomas in Neurofibromatosis Type 1. *J. Child Neurol.* 33, 73–81. <https://doi.org/10.1177/0883073817739509>

- Carpenter, E.L., Lau, H.A., Kolodny, E.H., Adler, R.S., 2015. Skeletal Muscle in Healthy Subjects versus Those with GNE-Related Myopathy: Evaluation with Shear-Wave US--A Pilot Study. *Radiology* 277, 546–554. <https://doi.org/10.1148/radiol.2015142212>
- Cartwright, M.S., Passmore, L.V., Yoon, J.-S., Brown, M.E., Caress, J.B., Walker, F.O., 2008. Cross-sectional area reference values for nerve ultrasonography. *Muscle Nerve* 37, 566–571. <https://doi.org/10.1002/mus.21009>
- Castle, D., Robertson, N.P., 2019. Alternatives to intravenous immunoglobulin treatment in chronic inflammatory demyelinating polyradiculoneuropathy. *J. Neurol.* 266, 2338–2340. <https://doi.org/10.1007/s00415-019-09485-9>
- Chino, K., Akagi, R., Dohi, M., Takahashi, H., 2014. Measurement of muscle architecture concurrently with muscle hardness using ultrasound strain elastography. *Acta Radiol. Stockh. Swed.* 1987 55, 833–839. <https://doi.org/10.1177/0284185113507565>
- Correas, J.M., Drakonakis, E., Isidori, A.M., Hélénon, O., Pozza, C., Cantisani, V., Di Leo, N., Maghella, F., Rubini, A., Drudi, F.M., D'ambrosio, F., 2013. Update on ultrasound elastography: miscellanea. Prostate, testicle, musculo-skeletal. *Eur. J. Radiol.* 82, 1904–1912. <https://doi.org/10.1016/j.ejrad.2013.05.031>
- Cortez, C.D., Hermitte, L., Romain, A., Mesmann, C., Lefort, T., Pialat, J.B., 2016. Ultrasound shear wave velocity in skeletal muscle: A reproducibility study. *Diagn. Interv. Imaging* 97, 71–79. <https://doi.org/10.1016/j.diii.2015.05.010>
- Cosgrove, D.O., Berg, W.A., Doré, C.J., Skyba, D.M., Henry, J.-P., Gay, J., Cohen-Bacrie, C., the BE1 Study Group, 2012. Shear wave elastography for breast masses is highly reproducible. *Eur. Radiol.* 22, 1023–1032. <https://doi.org/10.1007/s00330-011-2340-y>
- Creze, M., Nordez, A., Soubeyrand, M., Rocher, L., Maître, X., Bellin, M.-F., 2018. Shear wave sonoelastography of skeletal muscle: basic principles, biomechanical concepts, clinical applications, and future perspectives. *Skeletal Radiol.* 47, 457–471. <https://doi.org/10.1007/s00256-017-2843-y>
- Di Pasquale, A., Morino, S., Loreti, S., Bucci, E., Vanacore, N., Antonini, G., 2015. Peripheral nerve ultrasound changes in CIDP and correlations with nerve conduction velocity. *Neurology* 84, 803–809. <https://doi.org/10.1212/WNL.0000000000001291>
- Dietrich, C.F., Barr, R.G., Farrokh, A., Dighe, M., Hocke, M., Jenssen, C., Dong, Y., Saftoiu, A., Havre, R.F., 2017. Strain Elastography - How To Do It? *Ultrasound Int. Open* 3, E137–E149. <https://doi.org/10.1055/s-0043-119412>
- Dimachkie, M.M., Barohn, R.J., 2013. Chronic Inflammatory Demyelinating Polyneuropathy. *Curr. Treat. Options Neurol.* 15, 350–366. <https://doi.org/10.1007/s11940-013-0229-6>
- Donaghy, M., 2003. Enlarged Peripheral Nerves. *Pract. Neurol.* 3, 40–45. <https://doi.org/10.1046/j.1474-7766.2003.00121.x>
- Eby, S.F., Song, P., Chen, S., Chen, Q., Greenleaf, J.F., An, K.-N., 2013. Validation of shear wave elastography in skeletal muscle. *J. Biomech.* 46, 2381–2387. <https://doi.org/10.1016/j.jbiomech.2013.07.033>

- Eftimov, F., Lucke, I.M., Querol, L.A., Rajabally, Y.A., Verhamme, C., 2020. Diagnostic challenges in chronic inflammatory demyelinating polyradiculoneuropathy. *Brain J. Neurol.* 143, 3214–3224. <https://doi.org/10.1093/brain/awaa265>
- Eichelmann, K., González González, S.E., Salas-Alanis, J.C., Ocampo-Candiani, J., 2013. Leprosy. An update: definition, pathogenesis, classification, diagnosis, and treatment. *Actas Dermosifiliogr.* 104, 554–563. <https://doi.org/10.1016/j.adengl.2012.03.028>
- Epstein, J.I., Allsbrook, W.C., Amin, M.B., Egevad, L.L., ISUP Grading Committee, 2005. The 2005 International Society of Urological Pathology (ISUP) Consensus Conference on Gleason Grading of Prostatic Carcinoma. *Am. J. Surg. Pathol.* 29, 1228–1242. <https://doi.org/10.1097/01.pas.0000173646.99337.b1>
- Evans, Dg.R., 2009. Neurofibromatosis type 2 (NF2): A clinical and molecular review. *Orphanet J. Rare Dis.* 4, 16. <https://doi.org/10.1186/1750-1172-4-16>
- Evans, D.G.R., O'Hara, C., Wilding, A., Ingham, S.L., Howard, E., Dawson, J., Moran, A., Scott-Kitching, V., Holt, F., Huson, S.M., 2011. Mortality in neurofibromatosis 1: in North West England: an assessment of actuarial survival in a region of the UK since 1989. *Eur. J. Hum. Genet.* 19, 1187–1191. <https://doi.org/10.1038/ejhg.2011.113>
- Ewertsen, C., Carlsen, J.F., Christiansen, I.R., Jensen, J.A., Nielsen, M.B., 2016. Evaluation of healthy muscle tissue by strain and shear wave elastography - Dependency on depth and ROI position in relation to underlying bone. *Ultrasonics* 71, 127–133. <https://doi.org/10.1016/j.ultras.2016.06.007>
- Ferner, R., Huson, S., Thomas, N., Moss, C., Willshaw, H., Evans, D., Upadhyaya, M., Towers, R., Gleeson, M., Steiger, C., Kirby, A., 2007. Guidelines for the diagnosis and management of individuals with Neurofibromatosis 1 (NF1). *J. Med. Genet.* 44, 81–8. <https://doi.org/10.1136/jmg.2006.045906>
- Ferraioli, G., Wong, V.W.-S., Castera, L., Berzigotti, A., Sporea, I., Dietrich, C.F., Choi, B.I., Wilson, S.R., Kudo, M., Barr, R.G., 2018. Liver Ultrasound Elastography: An Update to the World Federation for Ultrasound in Medicine and Biology Guidelines and Recommendations. *Ultrasound Med. Biol.* 44, 2419–2440. <https://doi.org/10.1016/j.ultrasmedbio.2018.07.008>
- Gennisson, J.-L., Deffieux, T., Fink, M., Tanter, M., 2013. Ultrasound elastography: principles and techniques. *Diagn. Interv. Imaging* 94, 487–495. <https://doi.org/10.1016/j.diii.2013.01.022>
- Ghalayani, P., Saberi, Z., Sardari, F., 2012. Neurofibromatosis type I (von Recklinghausen's disease): A family case report and literature review. *Dent. Res. J.* 9, 483–488.
- Gong, X., Xu, Q., Xu, Z., Xiong, P., Yan, W., Chen, Y., 2011. Real-time elastography for the differentiation of benign and malignant breast lesions: a meta-analysis. *Breast Cancer Res. Treat.* 130, 11. <https://doi.org/10.1007/s10549-011-1745-2>

- Greening, J., Dilley, A., 2017. Posture-induced changes in peripheral nerve stiffness measured by ultrasound shear-wave elastography. *Muscle Nerve* 55, 213–222. <https://doi.org/10.1002/mus.25245>
- Grimm, A., Décard, B.F., Axer, H., Fuhr, P., 2015. The Ultrasound pattern sum score - UPSS. A new method to differentiate acute and subacute neuropathies using ultrasound of the peripheral nerves. *Clin. Neurophysiol. Off. J. Int. Fed. Clin. Neurophysiol.* 126, 2216–2225. <https://doi.org/10.1016/j.clinph.2015.01.011>
- Hall, T.J., Milkowski, A., Garra, B., Carson, P., Palmeri, M., Nightingale, K., Lynch, T., Alturki, A., Andre, M., Audiere, S., Bamber, J., Barr, R., Bercoff, Jeremy, Bercoff, Jessica, Bernal, M., Brum, J., Chan, H.W., Chen, S., Cohen-Bacrie, C., Couade, M., Daniels, A., Dewall, R., Dillman, J., Ehman, R., Franchi-Abella, S., Fromageau, J., Gennisson, J.L., Henry, J.P., Ivancevich, N., Kalin, J., Kohn, S., Kugel, J., Lee, K., Liu, N., Loupas, T., Mazernik, J., McAleavey, S., Miette, V., Metz, S., Morel, B., Nelson, T., Nordberg, E., Oudry, J., Padwal, M., Rouze, N., Samir, A., Sandrin, L., Schaccitti, J., Schmitt, C., Shamdasani, V., Song, P., Switalski, P., Wang, M., Wear, K., Xie, H., Zhao, H., 2013. RSNA/QIBA: 2013 IEEE International Ultrasonics Symposium, IUS 2013. 2013 IEEE Int. Ultrason. Symp. IUS 2013, IEEE International Ultrasonics Symposium, IUS 397–400. <https://doi.org/10.1109/ULTSYM.2013.0103>
- Hirst, C., Raasch, S., Llewelyn, G., Robertson, N., 2006. Remission of chronic inflammatory demyelinating polyneuropathy after alemtuzumab (Campath 1H). *J. Neurol. Neurosurg. Psychiatry* 77, 800–802. <https://doi.org/10.1136/jnnp.2005.076869>
- HOU, Y., ALLEN, T., WOLTERS, P.L., TOLEDO-TAMULA, M.A., MARTIN, S., BALDWIN, A., REDA, S., GILLESPIE, A., GOODWIN, A., WIDEMANN, B.C., 2020. Predictors of cognitive development in children with neurofibromatosis type 1 and plexiform neurofibromas. *Dev. Med. Child Neurol.* 62, 977–984. <https://doi.org/10.1111/dmcn.14489>
- Hu, X., Liu, Y., Qian, L., 2017. Diagnostic potential of real-time elastography (RTE) and shear wave elastography (SWE) to differentiate benign and malignant thyroid nodules: A systematic review and meta-analysis. *Medicine (Baltimore)* 96, e8282. <https://doi.org/10.1097/MD.00000000000008282>
- Ishibashi, F., Taniguchi, M., Kojima, R., Kawasaki, A., Kosaka, A., Uetake, H., 2016. Elasticity of the tibial nerve assessed by sonoelastography was reduced before the development of neuropathy and further deterioration associated with the severity of neuropathy in patients with type 2 diabetes. *J. Diabetes Investig.* 7, 404–412. <https://doi.org/10.1111/jdi.12408>
- Itoh, A., Ueno, E., Tohno, E., Kamma, H., Takahashi, H., Shiina, T., Yamakawa, M., Matsumura, T., 2006. Breast disease: clinical application of US elastography for diagnosis. *Radiology* 239, 341–350. <https://doi.org/10.1148/radiol.2391041676>
- Jacques, C., Dietemann, J.L., 2005. Imagerie de la neurofibromatose de type 1. *J. Neuroradiol.* 32, 180–197. [https://doi.org/10.1016/S0150-9861\(05\)83136-0](https://doi.org/10.1016/S0150-9861(05)83136-0)

- Kantarci, F., Ustabasioglu, F.E., Delil, S., Olgun, D.C., Korkmazer, B., Dikici, A.S., Tutar, O., Nalbantoglu, M., Uzun, N., Mihmanli, I., 2014. Median nerve stiffness measurement by shear wave elastography: a potential sonographic method in the diagnosis of carpal tunnel syndrome. *Eur. Radiol.* 24, 434–440. <https://doi.org/10.1007/s00330-013-3023-7>
- Khadilkar, S.V., Yadav, R.S., Soni, G., 2015. A practical approach to enlargement of nerves, plexuses and roots. *Pract. Neurol.* 15, 105–115. <https://doi.org/10.1136/practneurol-2014-001004>
- Kim, A., Gillespie, A., Dombi, E., Goodwin, A., Goodspeed, W., Fox, E., Balis, F.M., Widemann, B.C., 2009. Characteristics of children enrolled in treatment trials for NF1-related plexiform neurofibromas. *Neurology* 73, 1273–1279. <https://doi.org/10.1212/WNL.0b013e3181bd1326>
- Kim, S.H., Lee, J.M., Lee, M.W., Kim, G.H., Han, J.K., Choi, B.I., 2008. Sonography Transmission Gel as Endorectal Contrast Agent for Tumor Visualization in Rectal Cancer. *Am. J. Roentgenol.* 191, 186–189. <https://doi.org/10.2214/AJR.07.3067>
- Koike, H., Katsuno, M., 2020. Pathophysiology of Chronic Inflammatory Demyelinating Polyneuropathy: Insights into Classification and Therapeutic Strategy. *Neurol. Ther.* 9, 213–227. <https://doi.org/10.1007/s40120-020-00190-8>
- Koo, T.K., Li, M.Y., 2016. A Guideline of Selecting and Reporting Intraclass Correlation Coefficients for Reliability Research. *J. Chiropr. Med.* 15, 155–163. <https://doi.org/10.1016/j.jcm.2016.02.012>
- Korf, B.R., 2013a. Neurofibromatosis. *Handb. Clin. Neurol.* 111, 333–340. <https://doi.org/10.1016/B978-0-444-52891-9.00039-7>
- Korf, B.R., 2013b. Neurofibromatosis. *Handb. Clin. Neurol.* 111, 333–340. <https://doi.org/10.1016/B978-0-444-52891-9.00039-7>
- Kuk, J.L., Saunders, T.J., Davidson, L.E., Ross, R., 2009. Age-related changes in total and regional fat distribution. *Ageing Res. Rev.* 8, 339–348. <https://doi.org/10.1016/j.arr.2009.06.001>
- Kuo, T.-C., Wu, M.-H., Chen, K.-Y., Hsieh, M.-S., Chen, A., Chen, C.-N., 2020. Ultrasonographic features for differentiating follicular thyroid carcinoma and follicular adenoma. *Asian J. Surg.* 43, 339–346. <https://doi.org/10.1016/j.asjsur.2019.04.016>
- Lam, A.C.L., Pang, S.W.A., Ahuja, A.T., Bhatia, K.S.S., 2016. The influence of precompression on elasticity of thyroid nodules estimated by ultrasound shear wave elastography. *Eur. Radiol.* 26, 2845–2852. <https://doi.org/10.1007/s00330-015-4108-2>
- Learning disabilities in children with neurofibromatosis type 1: subtypes, cognitive profile, and attention-deficit-hyperactivity disorder - PubMed [WWW Document], n.d. URL <https://pubmed.ncbi.nlm.nih.gov/17109785/> (accessed 3.3.22).
- Lehmann, H.C., Burke, D., Kuwabara, S., 2019. Chronic inflammatory demyelinating polyneuropathy: update on diagnosis, immunopathogenesis and treatment. *J. Neurol. Neurosurg. Psychiatry* 90, 981–987. <https://doi.org/10.1136/jnnp-2019-320314>
- Leong, W., Lai, L., Nik Mustapha, N.R., Vijayanathan, A., Rahmat, K., Mahadeva, S., Chan, W.-K., 2019. Comparing point shear wave

- elastography (ElastPQ) and transient elastography for diagnosis of fibrosis stage in nonalcoholic fatty liver disease. *J. Gastroenterol. Hepatol.* 35. <https://doi.org/10.1111/jgh.14782>
- Liu, C., Li, T.T., Hu, Z., Li, Y., Cheng, X., Zhu, Y., Lu, M., 2019. Transvaginal Real-time Shear Wave Elastography in the Diagnosis of Cervical Disease. *J. Ultrasound Med. Off. J. Am. Inst. Ultrasound Med.* 38, 3173–3181. <https://doi.org/10.1002/jum.15018>
- Liu, F., Zhu, J., Wei, M., Bao, Y., Hu, B., 2012. Preliminary evaluation of the sural nerve using 22-MHz ultrasound: a new approach for evaluation of diabetic cutaneous neuropathy. *PloS One* 7, e32730. <https://doi.org/10.1371/journal.pone.0032730>
- Merlini, L., Vargas, M.I., Anooshiravani, M., Viallon, M., Fluss, J., Hanquinet, S., 2011. Look for the nerves! MR neurography adds essential diagnostic value to routine MRI in pediatric practice: a pictorial overview. *J. Neuroradiol.* 38, 141–147. <https://doi.org/10.1016/j.neurad.2010.09.006>
- Miettinen, M.M., Antonescu, C.R., Fletcher, C.D.M., Kim, A., Lazar, A.J., Quezado, M.M., Reilly, K.M., Stemmer-Rachamimov, A., Stewart, D.R., Viskochil, D., Widemann, B., Perry, A., 2017. HISTOPATHOLOGIC EVALUATION OF ATYPICAL NEUROFIBROMATOUS TUMORS AND THEIR TRANSFORMATION INTO MALIGNANT PERIPHERAL NERVE SHEATH TUMOR IN NEUROFIBROMATOSIS 1 PATIENTS – A CONSENSUS OVERVIEW. *Hum. Pathol.* 67, 1–10. <https://doi.org/10.1016/j.humpath.2017.05.010>
- Miraglia, E., Moliterni, E., Iacovino, C., Roberti, V., Laghi, A., Moramarco, A., Giustini, S., 2020. Cutaneous manifestations in neurofibromatosis type 1. *Clin. Ter.* 171, e371–e377. <https://doi.org/10.7417/CT.2020.2242>
- Murray, T.S., Shapiro, E.D., 2010. Lyme Disease. *Clin. Lab. Med.* 30, 311–328. <https://doi.org/10.1016/j.cll.2010.01.003>
- Nam, K., Peterson, S.M., Wessner, C.E., Machado, P., Forsberg, F., 2021. Diagnosis of Carpal Tunnel Syndrome using Shear Wave Elastography and High-frequency Ultrasound Imaging. *Acad. Radiol.* 28, e278–e287. <https://doi.org/10.1016/j.acra.2020.08.011>
- Neurofibromatosis 2 - GeneReviews® - NCBI Bookshelf [WWW Document], n.d. URL <https://www.ncbi.nlm.nih.gov/books/NBK1201/> (accessed 8.15.22).
- Nižetić, D., Groet, J., 2012. Tumorigenesis in Down’s syndrome: big lessons from a small chromosome. *Nat. Rev. Cancer* 12, 721–732. <https://doi.org/10.1038/nrc3355>
- Osterman, M., Draeger, R., Stern, P., 2014. Acute hand infections. *J. Hand Surg.* 39, 1628–1635; quiz 1635. <https://doi.org/10.1016/j.jhsa.2014.03.031>
- Ouiminga, H.A.K., Zabsonré, S.D., Kélani, A., Ouattara, S., Dravé, A., Kabore, R.M., Sankara, D.H., Gaye, M., 2019. Spinal Cord Compression, a Rare Neurofibromatosis Complication. *World J. Neurosci.* 9, 191–198. <https://doi.org/10.4236/wjns.2019.93012>
- Ozturk, M., Selcuk, M.B., Polat, A.V., Ozbalci, A.B., Baris, Y.S., 2020. The diagnostic value of ultrasound and shear wave elastography in the

- differentiation of benign and malignant soft tissue tumors. *Skeletal Radiol.* 49, 1795–1805. <https://doi.org/10.1007/s00256-020-03492-y>
- Reynolds, D.L., Jacobson, J.A., Inampudi, P., Jamadar, D.A., Ebrahim, F.S., Hayes, C.W., 2004. Sonographic Characteristics of Peripheral Nerve Sheath Tumors. *Am. J. Roentgenol.* 182, 741–744. <https://doi.org/10.2214/ajr.182.3.1820741>
- Riazi, S., Bril, V., Perkins, B.A., Abbas, S., Chan, V.W.S., Ngo, M., Lovblom, L.E., El-Beheiry, H., Brull, R., 2012. Can ultrasound of the tibial nerve detect diabetic peripheral neuropathy? A cross-sectional study. *Diabetes Care* 35, 2575–2579. <https://doi.org/10.2337/dc12-0739>
- Rugel, C.L., Franz, C.K., Lee, S.S.M., 2020. Influence of limb position on assessment of nerve mechanical properties by using shear wave ultrasound elastography. *Muscle Nerve* 61, 616–622. <https://doi.org/10.1002/mus.26842>
- Ruggieri, M., Praticò, A.D., Serra, A., Maiolino, L., Cocuzza, S., Di Mauro, P., Licciardello, L., Milone, P., Privitera, G., Belfiore, G., Di Pietro, M., Di Raimondo, F., Romano, A., Chiarenza, A., Muglia, M., Polizzi, A., Evans, D.G., 2016. Childhood neurofibromatosis type 2 (NF2) and related disorders: from bench to bedside and biologically targeted therapies. *Acta Otorhinolaryngol. Ital.* 36, 345–367. <https://doi.org/10.14639/0392-100X-1093>
- Saito, K., Kato, M., Susaki, N., Nagatani, T., Nagasaka, T., Yoshida, J., 2003. Expression of Ki-67 antigen and vascular endothelial growth factor in sporadic and neurofibromatosis type 2-associated schwannomas. *Clin. Neuropathol.* 22, 30–34.
- Senthilkumar, V.A., Tripathy, K., 2023. Lisch Nodules, in: *StatPearls*. StatPearls Publishing, Treasure Island (FL).
- Sepe, A., Tchkonja, T., Thomou, T., Zamboni, M., Kirkland, J.L., 2011. Aging and regional differences in fat cell progenitors - a mini-review. *Gerontology* 57, 66–75. <https://doi.org/10.1159/000279755>
- Shear wave elastography of the saphenous nerve : Medicine [WWW Document], n.d. URL https://journals.lww.com/md-journal/Fulltext/2020/09110/Shear_wave_elastography_of_the_saphenous_nerve.52.aspx (accessed 9.3.22).
- Shoji, S., Hashimoto, A., Nakamura, T., Hiraiwa, S., Sato, H., Sato, Y., Tajiri, T., Miyajima, A., 2018. Novel application of three-dimensional shear wave elastography in the detection of clinically significant prostate cancer. *Biomed. Rep.* 8, 373–377. <https://doi.org/10.3892/br.2018.1059>
- Simanshu, D.K., Nissley, D.V., McCormick, F., 2017. RAS Proteins and Their Regulators in Human Disease. *Cell* 170, 17–33. <https://doi.org/10.1016/j.cell.2017.06.009>
- Spina, E., Topa, A., Iodice, R., Tozza, S., Ruggiero, L., Dubbioso, R., Esposito, M., Bruzzese, D., Santoro, L., Manganelli, F., 2017. Early predictive factors of disability in CIDP. *J. Neurol.* 264, 1–6. <https://doi.org/10.1007/s00415-017-8578-9>
- Staber, D., Oppold, J., Grimm, A., Schuhmann, M.U., Romano, A., Marquetand, J., Kleiser, B., 2022. Shear-Wave-Elastography in Neurofibromatosis Type I. *Diagnostics* 12, 360. <https://doi.org/10.3390/diagnostics12020360>

- Stangerup, S.-E., Caye-Thomasen, P., Tos, M., Thomsen, J., 2006. The natural history of vestibular schwannoma. *Otol. Neurotol. Off. Publ. Am. Otol. Soc. Am. Neurotol. Soc. Eur. Acad. Otol. Neurotol.* 27, 547–552. <https://doi.org/10.1097/01.mao.0000217356.73463.e7>
- Suarez-Kelly, L.P., Yu, L., Kline, D., Schneider, E.B., Agnese, D.M., Carson, W.E., 2019. Increased breast cancer risk in women with neurofibromatosis type 1: a meta-analysis and systematic review of the literature. *Hered. Cancer Clin. Pract.* 17, 12. <https://doi.org/10.1186/s13053-019-0110-z>
- Surace, E.I., Haippek, C.A., Gutmann, D.H., 2004. Effect of merlin phosphorylation on neurofibromatosis 2 (NF2) gene function. *Oncogene* 23, 580–587. <https://doi.org/10.1038/sj.onc.1207142>
- Taljanovic, M.S., Gimber, L.H., Becker, G.W., Latt, L.D., Klauser, A.S., Melville, D.M., Gao, L., Witte, R.S., 2017. Shear-Wave Elastography: Basic Physics and Musculoskeletal Applications. *Radiogr. Rev. Publ. Radiol. Soc. N. Am. Inc* 37, 855–870. <https://doi.org/10.1148/rg.2017160116>
- Tang, X., Wang, L., Guo, R., Huang, S., Tang, Y., Qiu, L., 2020. Application of ultrasound elastography in the evaluation of muscle strength in a healthy population. *Quant. Imaging Med. Surg.* 10, 1961–1972. <https://doi.org/10.21037/qims-20-439>
- Van den Bergh, P.Y.K., van Doorn, P.A., Hadden, R.D.M., Avau, B., Vankrunkelsven, P., Allen, J.A., Attarian, S., Blomkwist-Markens, P.H., Cornblath, D.R., Eftimov, F., Goedee, H.S., Harbo, T., Kuwabara, S., Lewis, R.A., Lunn, M.P., Nobile-Orazio, E., Querol, L., Rajabally, Y.A., Sommer, C., Topaloglu, H.A., 2021. European Academy of Neurology/Peripheral Nerve Society guideline on diagnosis and treatment of chronic inflammatory demyelinating polyradiculoneuropathy: Report of a joint Task Force-Second revision. *J. Peripher. Nerv. Syst. JPNS* 26, 242–268. <https://doi.org/10.1111/jns.12455>
- Wee, T.C., Simon, N., 2020. Shearwave Elastography in the Differentiation of Carpal Tunnel Syndrome Severity. *PM&R* 12. <https://doi.org/10.1002/pmrj.12334>
- Wei, M., Ye, X., 2020. Feasibility of Point Shear Wave Elastography for Evaluating Diabetic Peripheral Neuropathy. *J. Ultrasound Med. Off. J. Am. Inst. Ultrasound Med.* 39, 1135–1141. <https://doi.org/10.1002/jum.15198>
- Well, L., Jaeger, A., Kehrer-Sawatzki, H., Farschtschi, S., Avanesov, M., Sauer, M., Sousa, M.T. de, Bannas, P., Derlin, T., Adam, G., Mautner, V.F., Salamon, J.M., 2020. The effect of pregnancy on growth-dynamics of neurofibromas in Neurofibromatosis type 1. *PLOS ONE* 15, e0232031. <https://doi.org/10.1371/journal.pone.0232031>
- Winter, N., Rattay, T.W., Axer, H., Schäffer, E., Décard, B.F., Gugel, I., Schuhmann, M., Grimm, A., 2017. Ultrasound assessment of peripheral nerve pathology in neurofibromatosis type 1 and 2. *Clin. Neurophysiol. Off. J. Int. Fed. Clin. Neurophysiol.* 128, 702–706. <https://doi.org/10.1016/j.clinph.2017.02.005>

- Woo, S., Kim, S.Y., Cho, J.Y., Kim, S.H., 2014. Shear Wave Elastography for Detection of Prostate Cancer: A Preliminary Study. *Korean J. Radiol.* 15, 346–355. <https://doi.org/10.3348/kjr.2014.15.3.346>
- Zaidman, C.M., Al-Lozi, M., Pestronk, A., 2009. Peripheral nerve size in normals and patients with polyneuropathy: an ultrasound study. *Muscle Nerve* 40, 960–966. <https://doi.org/10.1002/mus.21431>
- Zaidman, C.M., Pestronk, A., 2014a. Nerve size in chronic inflammatory demyelinating neuropathy varies with disease activity and therapy response over time: a retrospective ultrasound study. *Muscle Nerve* 50, 733–738. <https://doi.org/10.1002/mus.24227>
- Zaidman, C.M., Pestronk, A., 2014b. Nerve Size in CIDP Varies with Disease Activity and Therapy Response Over Time: A Retrospective Ultrasound Study. *Muscle Nerve* 50, 733–738. <https://doi.org/10.1002/mus.24227>
- Zaki, M., Hazem, M., Elsamman, M., 2019. Shear wave elastography in assessment of liver stiffness and prediction of gastro-esophageal varices in patients with liver cirrhosis. *Egypt. J. Radiol. Nucl. Med.* 50, 16. <https://doi.org/10.1186/s43055-019-0015-x>
- Zhong, L.-C., Yang, T., Gu, L.-P., Ma, F., 2021. The diagnostic performance of shear wave velocity ratio for the differential diagnosis of benign and malignant breast lesions: Compared with VTQ, and mammography. *Clin. Hemorheol. Microcirc.* 77, 123–131. <https://doi.org/10.3233/CH-200813>
- Zhu, B., Yan, F., He, Y., Wang, L., Xiang, X., Tang, Y., Yang, Y., Qiu, L., 2018. Evaluation of the healthy median nerve elasticity: Feasibility and reliability of shear wave elastography. *Medicine (Baltimore)* 97, e12956. <https://doi.org/10.1097/MD.00000000000012956>

7. Declaration of own contribution

All data was collected in the Department of Neurology in Tübingen at the University Hospital under the supervision of my supervisor Dr. MD Justus Marquetand.

The conception of this study was carried out by / in collaboration with my mentor, Dr. med. Justus Marquetand.

The experiments were carried out by me after having received training from Dr. med. Justus Marquetand.

The statistical analysis was performed independently by me.

I can confirm that I have written the manuscript independently and no other sources were used other than those indicated by me.

Deborah Staber 21.02.24

8. Own Publications

Staber, D., Oppold, J., Grimm, A., Schuhmann, M.U., Romano, A., Marquetand, J., Kleiser, B., 2022. Shear-Wave-Elastography in Neurofibromatosis Type I. *Diagnostics* 12, 360. <https://doi.org/10.3390/diagnostics12020360>

9. Acknowledgements

I would like to thank my mentor, Justus, for his patience and humour throughout this thesis. I would also like to thank my friends and family but also myself for helping me stay positive throughout this process.

The methodological advice of the Institute for Clinical Epidemiology and Applied Biometry at the University of Tübingen was utilized for this work. I would like to thank Dr. You-Fang Sheng for their support.